

Design and Manufacturing of HydRotor

A Final Year Project Report

Presented to

SCHOOL OF MECHANICAL & MANUFACTURING ENGINEERING

Department of Mechanical Engineering

NUST

ISLAMABAD, PAKISTAN

In Partial Fulfillment

of the Requirements for the Degree of

Bachelors of Mechanical Engineering

by

Mohammad Ali Yaqteen

Muhammad Azeem Ali

Sarmad Saleem

June 2018

EXAMINATION COMMITTEE

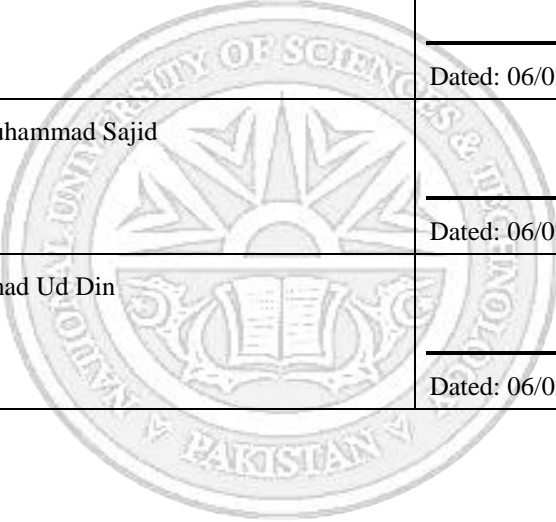
We hereby recommend that the final year project report prepared under our supervision by:

Mohammad Ali Yaqteen NUST201434387BSMME11114F.

Muhammad Azeem Ali NUST201434963BSMME11114F.

Sarmad Saleem NUST2014 32972BSMME11114F.

Titled: "Design and Manufacturing of HydRotor" be accepted in partial fulfillment of the requirements for the award of DEGREE NAME degree.

| | |
|---|--|
| Supervisor: AP Dr. Zaib Ali SMME NUST |  Dated: 06/02/2018 |
| Committee Member: AP Dr. Muhammad Sajid SMME, NUST | Dated: 06/02/2018 |
| Committee Member: AP Dr. Emad Ud Din SMME,NUST | Dated: 06/02/2018 |

(Head of Department)

(Date)

COUNTERSIGNED

Dated: _____

(Dean / Principal)

ABSTRACT

This work presented here describes the design of a power generation system that could be used in open channel water flow with low flow velocities. The purpose is to make a turbine that could provide for the power requirements of general public when on an adventurous trip or for a small scale power requirement in a forest. Experiments are done to find out whether setting up such a system in open channel water flow will actually be successful. small capacity power generation system is the aim, hence the name Hydrotor Turbine, and to discover new way of providing electricity to the people. To design such a system, a detailed study of different types of turbines is conducted. Vertical axis drag type turbines are most suited for small capacity generation systems. Therefore, a Savonius type water turbine is designed using helical blades to give the best possible results. A small prototype of the selected rotor is designed. Mathematical modeling of the turbine is completed after the design is finalized. The turbine is then 3D-printed in parts to maximum precision. The fabricated model is tested in the water tunnel to compare its results with the theoretical study done earlier. The turbine is portable and can simply be taken anywhere easily.

PREFACE

A turbine converts energy in the flowing water into rotating shaft power. The selection of the best turbine for any particular hydro site depends on the site characteristics, the dominant ones being the head, flow velocity and flow rate available. Selection also depends on the desired running speed of the generator or other device loading the turbine. Other considerations such as whether the turbine is expected to produce power under part-flow conditions also play an important role in the selection. All turbines have a power-speed characteristic. They will tend to run most efficiently at a particular speed, head and flow combination.

A turbine design speed is largely determined by the head under which it operates. Turbines can be classified as high head, medium head or low head machines. Turbines are also divided by their principle way of operating and can be either impulse or reaction turbines. This report is our work on how to design a hydrotor into a portable device.

ACKNOWLEDGMENTS

First of all, we would thank ALLAH Almighty, who gave us knowledge and dedication to be able to complete this research. We would also thank our Faculty advisor Dr. Zaib Ali and co-faculty advisors Dr. M. Sajid and Dr. Emad who, at each and every step, assisted us, encouraged us and guided us to complete the project successfully.

Last but not the least the project was possible because of the prayers and motivation that our parents put in for us. We dedicate our project to our parents.

ORIGINALITY REPORT

FYP

ORIGINALITY REPORT

15%

SIMILARITY INDEX

6%

INTERNET SOURCES

8%

PUBLICATIONS

9%

STUDENT PAPERS

PRIMARY SOURCES

| | | |
|----------|---|-----------|
| 1 | Submitted to British University in Egypt Student Paper | 3% |
| 2 | Anuj Kumar, R.P. Saini. "Performance parameters of Savonius type hydrokinetic turbine – A Review", Renewable and Sustainable Energy Reviews, 2016 Publication | 2% |
| 3 | www.slideshare.net Internet Source | 1% |
| 4 | Submitted to Indian Institute of Technology, Madras Student Paper | 1% |
| 5 | Kailash, Golecha, T. I. Eldho, and S. V. Prabhu. "Performance Study of Modified Savonius Water Turbine with Two Deflector Plates", International Journal of Rotating Machinery, 2012. Publication | 1% |
| 6 | Submitted to Eastern Mediterranean University Student Paper | 1% |

COPYRIGHT

- Copyright in text of this thesis rests with the student author. Copies (by any process) either in full, or of extracts, may be only in accordance with the instructions given by author and lodged in the Library of SMME, NUST. Details may be obtained by the librarian. This page must be part of any such copies made. Further copies (by any process) of copies made in accordance with such instructions may not be made without the permission (in writing) of the author.
- The ownership of any intellectual property rights which may be described in this thesis is vested in SMME, NUST, subject to any prior agreement to the contrary, and may not be made available for use of third parties without the written permission of SMME, NUST which will describe the terms and conditions of any such agreement.
- Further information on the conditions under which disclosure and exploitation may take place is available from the library of SMME, NUST Islamabad.

1 TABLE OF CONTENTS

| | |
|------------------------------|---|
| Chapter 1: Introduction | |
| 1.1 | Turbine 1 |
| 1.2 | Principle Types of Turbines 1 |
| 1.2.1 | Impulse Turbines: 1 |
| 1.2.2 | Reaction Turbines: 1 |
| 1.3 | Turbine types based on axis of rotation 2 |
| 1.3.1 | Horizontal axis turbines 2 |
| 1.3.2 | Vertical Axis turbines 2 |
| 1.3.3 | Types of VA Turbines 3 |
| 1.3.4 | Drag based VAT 3 |
| 1.3.5 | Lift based VAT 3 |
| 1.4 | Background 4 |
| 1.5 | Aims and Objectives 6 |
| 1.6 | Research methodology 6 |
| 1.7 | Concept Design 8 |
| Chapter 2: Literature Review | |
| 2.1 | General Lift and Drag Forces 9 |
| 2.1.1 | Lift Force 10 |
| 2.1.2 | Drag force 12 |
| 2.2 | Comparison between Vertical and Horizontal Axis Turbines 13 |
| 2.3 | Savonius Hydrokinetic Trubine 15 |
| 2.4 | Design Parameters 17 |
| 2.4.1 | Aspect Ratio 17 |
| 2.4.2 | End Plate 18 |
| 2.4.3 | Overlap Ratio 20 |
| 2.4.4 | Number of blades 22 |
| 2.4.5 | Multi Staging 25 |
| 2.4.6 | Deflector Plate 27 |
| 2.4.7 | Rotor Angle 28 |
| 2.4.8 | Reynold Number 28 |
| 2.4.9 | Tip Speed Ratio (TSR) 29 |
| 2.4.10 | Installation Parameter 29 |

Chapter 3: Methodology

| | | |
|-------|-----------------------------------|----|
| 3.1 | Design..... | 31 |
| 3.1.1 | Dimensions | 31 |
| 3.1.2 | 2-D Drawings | 32 |
| 3.1.3 | 3-D Model of Rotor | 32 |
| 3.1.4 | Bearing Housing | 33 |
| 3.1.5 | Frame Assembly | 33 |
| 3.1.6 | Assembly | 34 |
| 3.2 | Mathematical Model..... | 35 |
| 3.2.1 | Coefficient of Power..... | 35 |
| 3.2.2 | Power Available..... | 35 |
| 3.2.3 | Power Generated..... | 35 |
| 3.2.4 | Swept Area | 36 |
| 3.2.5 | Tip Speed Ratio (TSR) | 36 |
| 3.2.6 | Torque Coefficient (C_t)..... | 37 |
| 3.2.7 | Torque Available | 37 |
| 3.2.8 | Required Torque | 37 |
| 3.2.9 | Force Available..... | 37 |
| 3.3 | Ansys Fluent Simulation | 38 |

Chapter 4: Results & Discussions

| | | |
|-------|--|----|
| 4.1 | Theoretical..... | 39 |
| 4.2 | Manufacturing | 45 |
| 4.2.1 | 3D Printing | 45 |
| 4.2.2 | Side plates and Frame Fabrication..... | 45 |
| 4.2.3 | Rotor Assembly | 45 |
| 4.2.4 | Power Generation Assembly | 45 |
| 4.2.5 | Calculations and testing..... | 46 |

Chapter 5: Conclusion & Recommendations

| | | |
|-------|----------------------------------|----|
| 5.1 | Conclusion..... | 47 |
| 5.1.1 | Generator Drive Mechanism: | 47 |
| 5.1.2 | Material:..... | 47 |
| 5.1.3 | Performance:..... | 47 |
| 5.2 | Recommendations | 48 |

LIST OF FIGURES

| | |
|---|----|
| Figure 1: Savonius Turbine (D.Anderson, 2007)..... | 3 |
| Figure 2: Lift Based Turbine (D.Anderson, 2007)..... | 3 |
| Figure 3: Classification of Hydrokinetic Turbines..... | 5 |
| Figure 4: Overall Schematic of Research Methodology | 7 |
| Figure 5: Blade Design..... | 8 |
| Figure 6: Turbine Assembly..... | 8 |
| Figure 7: Darrieus and Savonius combination turbine (D.Anderson, 2007)..... | 9 |
| Figure 8: Pressure Distribution on an Airfoil (ManWell, 2002) | 10 |
| Figure 9: Basic shape of Savonius Rotor | 15 |
| Figure 10: A typical two bladed Savonius rotor..... | 16 |
| Figure 11: Betz Limits..... | 16 |
| Figure 12: Helical Savonius rotors with various shapes and sizes of end plates | 19 |
| Figure 13: Power coefficient of helical savonius wind turbines with end plates of various shapes and size | 19 |
| Figure 14: Variation of power coefficient with respect to TSR for two and three bladed rotor | 24 |
| Figure 15: Comparison between two and three stage rotors for static torque coefficient..... | 26 |
| Figure 16: Schematic of modified Savonius rotor with space parameters of deflector plate..... | 27 |
| Figure 17: Representation of rotor angle..... | 28 |
| Figure 18: Performance for CW | 30 |
| Figure 19: Performance for CCW | 30 |
| Figure 20: Max Power Coefficient vs Clearance Ratio..... | 30 |
| Figure 21: 2D Sketch of Rotor | 32 |
| Figure 22: 2 Stage - Helical Rotor..... | 32 |
| Figure 23: Bearing Housing | 33 |
| Figure 24: Frame Assembly | 33 |
| Figure 25: 3D Assembly of Turbine..... | 34 |
| Figure 26:Scheme of a Savonius rotor showing the tip velocity of the rotor..... | 36 |
| Figure 27: 2D design of the turbine with a large external enclosure Error! Bookmark not defined. | |
| Figure 28: Mesh generated in Ansys | 38 |

| | |
|---|----|
| Figure 29: Savonius Turbine with zero Overlap | 39 |
| Figure 30: Savonius Turbine with an overlap ratio of 0.242..... | 40 |
| Figure 31: Savonius Turbine with deflector and overlap ratio of 0.242 | 41 |
| Figure 32: Effect of Overlap Ratio..... | 42 |
| Figure 33: Effect of Deflector | 43 |
| Figure 34: Velocity Contour..... | 44 |

LIST OF TABLES

| | |
|---|----|
| Table 1: Comparison between Axial flow and Cross flow turbines..... | 13 |
| Table 2: C_p Results with different Aspect Ratios..... | 18 |
| Table 3: Effect of Overlap Ratio | 20 |
| Table 4: No. of blades vs C_p | 22 |
| Table 5: Stages vs C_p | 25 |
| Table 6: Geometric parameters for deflector plate positioning..... | 27 |

NOMENCLATURE

| <u>Symbol</u> | <u>Description</u> | <u>Unit</u> |
|---------------|--------------------------------|----------------------|
| ϕ | Angle of Attack | [$^{\circ}$] |
| θ | Angle of point of Force action | [$^{\circ}$] |
| μ | Dynamic Viscosity | [kg/m ³] |
| ω | Angular Velocity | [rad/s] |
| ρ | Density | [kg/m ³] |
| A_s | Swept Area | [m ²] |
| C_D | Drag Coefficient | [-] |
| C_P | Power Coefficient | [-] |
| C_t | Torque Coefficient | [-] |
| D | Diameter | [m] |
| F_A | Available Force | [N] |
| T | Torque | [N.m] |
| T_A | Torque Available | [N.m] |
| λ | Tip-Speed Ratio | [-] |
| H/L | Height | [m] |
| P | Power | [W] |
| P_A | Power Available | [W] |
| Re | Reynolds Number | [-] |

CHAPTER 1: INTRODUCTION

1.1 TURBINE

A turbine is a machine with at least one moving part called a rotor assembly, which is a shaft or drum with blades attached. Moving fluid acts on the blades so that they move and impart rotational energy to the rotor.

And hydro turbine is a machine that uses water kinetic or potential energy to rotate its blades and convert that energy to rotation energy.

Following is the brief introduction to different types of turbines with different perspectives;

1.2 PRINCIPLE TYPES OF TURBINES

1. Impulse Turbines
2. Reaction Turbines

1.2.1 Impulse Turbines:

Kinetic energy of a jet of water is converted into mechanical energy by impulse turbines. The impulse turbine generally **uses the velocity of the water** to move the runner and discharges to atmospheric pressure. The water stream hits each bucket on the runner. There is no suction on the down side of the turbine, and the water flows out the bottom of the turbine housing after hitting the runner. An impulse turbine is generally suitable for **high head, low flow** applications. Impulse turbines tolerate sand, are Easy to fabricate, efficient at wide a range of head and flow. Nozzle converts pressurized water into a high-speed jet of water.

1.2.2 Reaction Turbines:

Potential energy in pressurized water is converted into mechanical energy by reaction turbines. In a reaction turbine, the blades sit in a much larger volume of fluid and turn around as the fluid flows past them. Direction of the fluid flow is not changed by a reaction turbine as drastically as by impulse turbine: it simply spins as the fluid pushes through and past its blades.

Wind turbines are perhaps the most familiar examples of reaction turbines. If an impulse turbine is a bit like kicking soccer balls, a reaction turbine is more like swimming; in reverse. To better understand this think of how you do freestyle (front crawl) by hauling your arms through the water, starting with each hand as far in front as you can reach and ending with a "follow through" that throws your arm well behind you. What you're trying to achieve is to keep your hand and forearm pushing against the water for as long as possible, so you transfer as much energy as you can in each stroke. A reaction turbine is using the same idea in reverse: imagine fast-flowing water moving past you so it makes your arms and legs move and supplies energy to your body! With a reaction turbine, you want the water to touch the blades smoothly, for as long as it can, so it gives up as much energy as possible. The water isn't hitting the blades and bouncing off, as it does in an impulse turbine: instead, the blades are moving more smoothly, "going with the flow."

1.3 TURBINE TYPES BASED ON AXIS OF ROTATION

There are two types of turbine if we categorize due to their axis of rotation

1. Horizontal axis turbines
2. Vertical axis turbines

1.3.1 Horizontal axis turbines

Rotational axis of turbine is parallel to the flow direction. Conventional horizontal axis wind turbines are lift-based machines.

1.3.2 Vertical Axis turbines

Rotational axis of turbine is perpendicular to the flow direction. This kind of turbine is sometimes called "cross-flow turbine", as the turbine in principle also can be tilted 90 degrees to have a horizontal axis while still having its rotational axis perpendicular to the flow [31].

1.3.3 TYPES OF VA TURBINES

VA turbines can be categorized in two broad categories based on their working principle.

1. Drag based VAT
2. Lift Based VAT

1.3.4 Drag based VAT

Drag based vertical axis turbines apply force in the direction of relative flow. Drag-based devices **rely on variation of the drag coefficient** with respect to the orientation of the object. To create a reasonably efficient drag-based turbine, the drag coefficient should be high in one direction and low in the opposite direction, which gives a torque on the turbine. Drag-based devices achieve lower power coefficients than the lift-based but yields high torque.

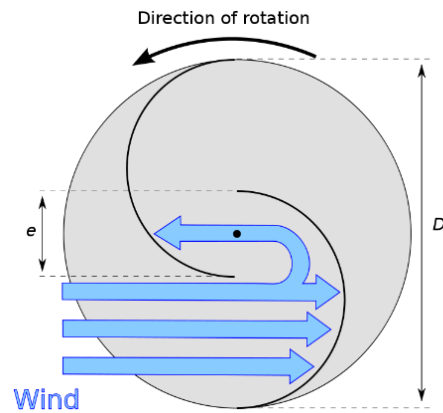


Figure 1: Savonius Turbine (D.Anderson, 2007)

1.3.5 Lift based VAT

Lift based VA turbines apply force perpendicular to the direction of relative flow. Main types of lift based VAT include Darrieus turbines, H-rotor turbines, Gorlov helical turbines. Lift-based turbine was originally invented by the French engineer George Jean Marie Darrieus in the 1920's. The patent

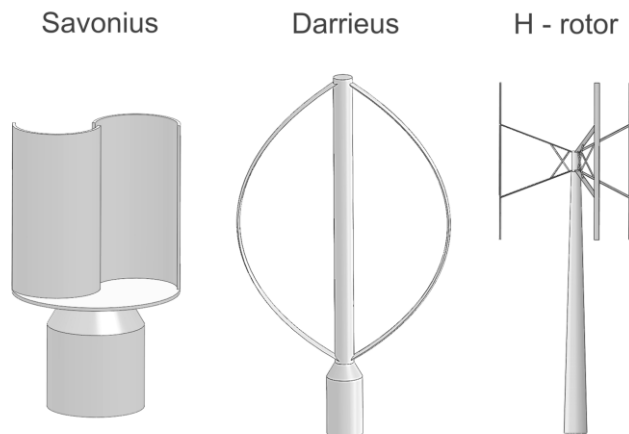


Figure 2: Lift Based Turbine (D.Anderson, 2007)

application of Darrieus covers the curved blade turbine and the H-rotor, as well as turbines with varying pitch angle and ducted turbines. It is suggested in the patent that the designs work both for wind and tidal energy. The aim of the curved blade design is to reduce the bending stresses in the blades due to centrifugal forces.

1.4 BACKGROUND

From earliest recorded periods of human history, mankind has been in a constant search to find, develop, and exploit ways to harness forces of nature present around him. Due to its relative conspicuousness, availability over a wide range of geographical terrains, ease of access, and raw force contained therein, the Hydro Power understandably became the most widely adopted source of extracting energy. Water current turbines are the main source of utilizing kinetic energy of natural water resources using different types of rotors. These rotors are either fixed to a structure on riverside or on floating pontoons. This type of power producing source is more reliable than other small power producing sources like solar and other etc. These hydro power turbines can be used to provide power to remote areas, or may be used to light a camp on river side. These types of hydro turbines are more preferable in the developing countries like Pakistan. There are different designs of water turbines for the extraction of energy from the water streams.

Based on the orientation of rotor axis with respect to water flow, these rotors are classified into two categories:

1. Vertical axis turbines (cross flow turbines)
2. Horizontal axis turbines (axial turbines).

Based on the pressure changes across the turbine blades hydraulic turbines are classified in two categories:

1. Impulse turbine works on the velocity of flowing water: The pressure of liquid does not change while flowing through the rotor of the machine.
2. Reaction turbine utilizes the head of the water for rotation: The pressure of liquid changes while it flows through the rotor of the machine [28].

Following is a demonstration of how hydrokinetic turbines are classified;

Horizontal axis turbines are expensive for small power generation. For small scale power generation, vertical axis turbines are most economical as they are less expensive and require less maintenance. Savonius, Darrieus and Gorlov helical water turbines are common types of savonius water turbines.

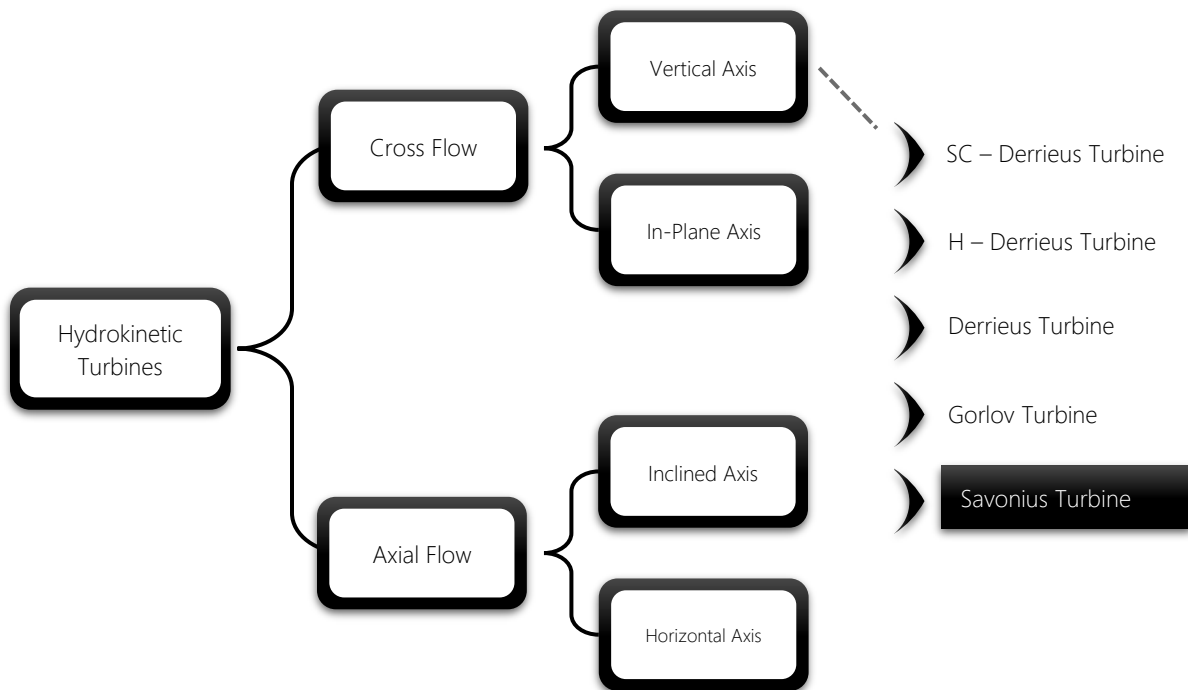


Figure 3: Classification of Hydrokinetic Turbines

In this project, modified savonius turbine are worked upon. **Savonius turbines are drag type turbines** as drag force is the main driving force for the operation of savonius type turbines [1]. It has S shaped blades and it is simple in construction. Using savonius rotor in river and canal streams has many advantages as fixed flow direction and effective use of deflector plate.

We are working turbine to improve power output. It is a two stage helical savonius turbine with 180° twist angle of its blades and 90° phase shift between stages. To further enhance performance, we are using deflector plate at an angle of 101° [29].

1.5 AIMS AND OBJECTIVES

Aim is to study different types of hydro-turbines, compare these designs against performance, adaptability to environment and cost of production. Our objective is to design a water turbine that can best utilize the hydro energy of slow moving water streams. Following are some basic objectives of our project;

- I. Designing a Hydro Turbine that is suited to the environmental conditions of Pakistan and can easily be manufactured and installed in urban as well as the rural settings.
- II. Saving the cost of Manufacturing substantially low so as to make it economically viable for domestic users and widely adoptable without compromising over its durability and operation.
- III. Designing and Manufacturing a Hydro Turbine that maximizes efficiency by tweaking and optimizing relevant variables such as blade radius, aspect ratio and overlap ratio etc.
- IV. Actual testing and evaluation of the prototype for validation.

1.6 RESEARCH METHODOLOGY

Before working on the project the first step is to gather information and then design that project. And same way while designing hydrator, the first step in the process is to understand the basic concept of the turbine design and the mathematical model that determines the performance outputs of the turbine by completely studying the literature present on the turbines and decide the most suited type of turbine available for the project. After selecting the type, the different design parameters of the turbine are investigated as to how their change affected the outcome. The best

understandable option is chosen. A schematic of overall research methodology is shown in following diagram;

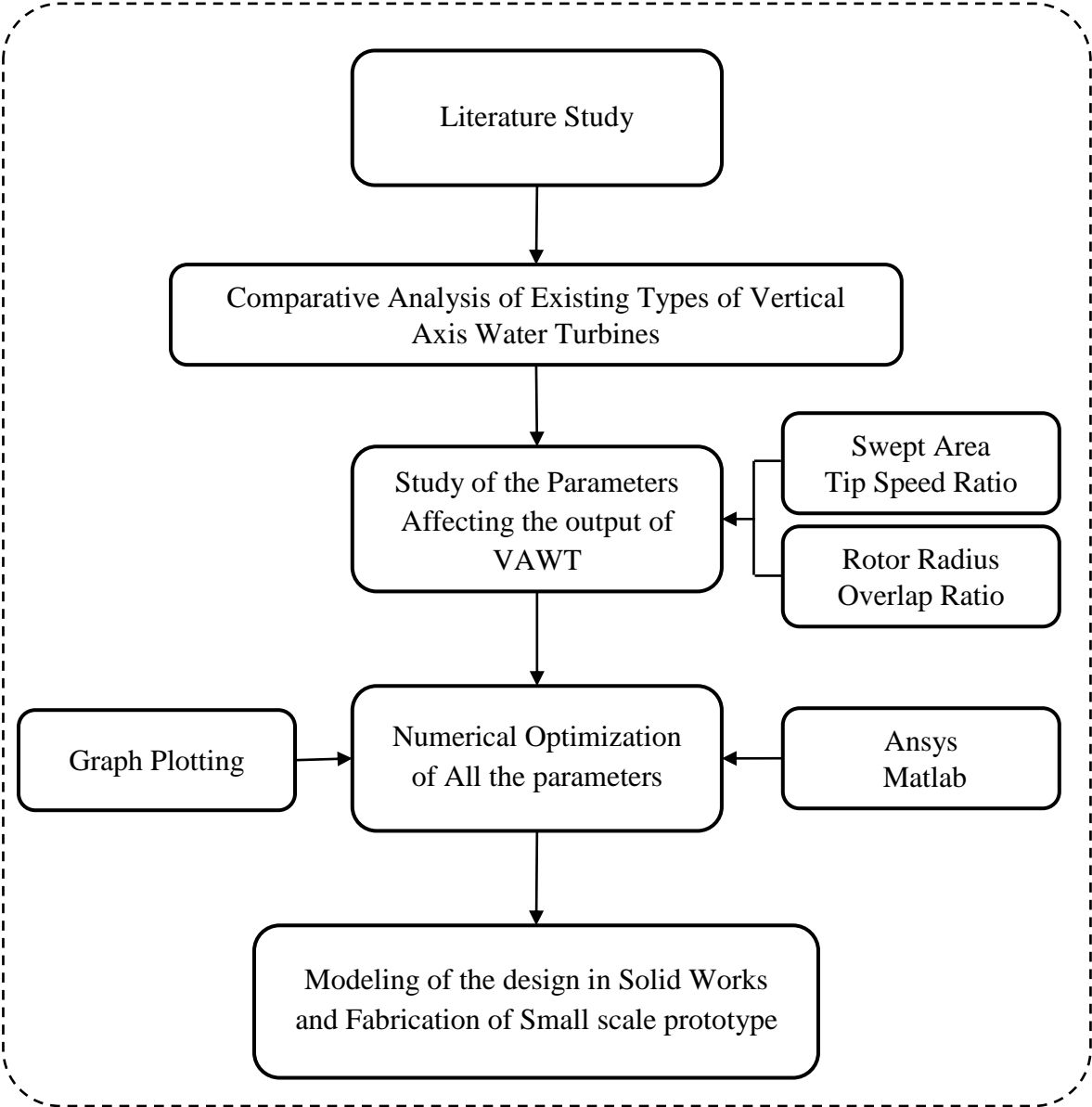


Figure 4: Overall Schematic of Research Methodology

1.7 CONCEPT DESIGN

Following pictures show the design concept of hydrotor;

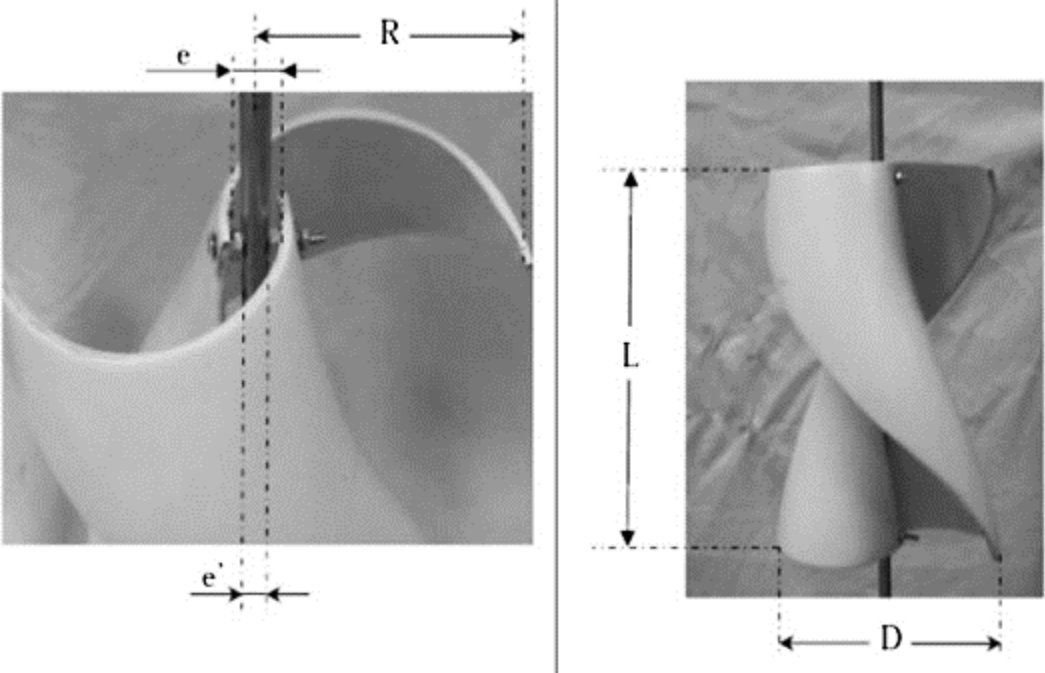


Figure 5: Blade Design

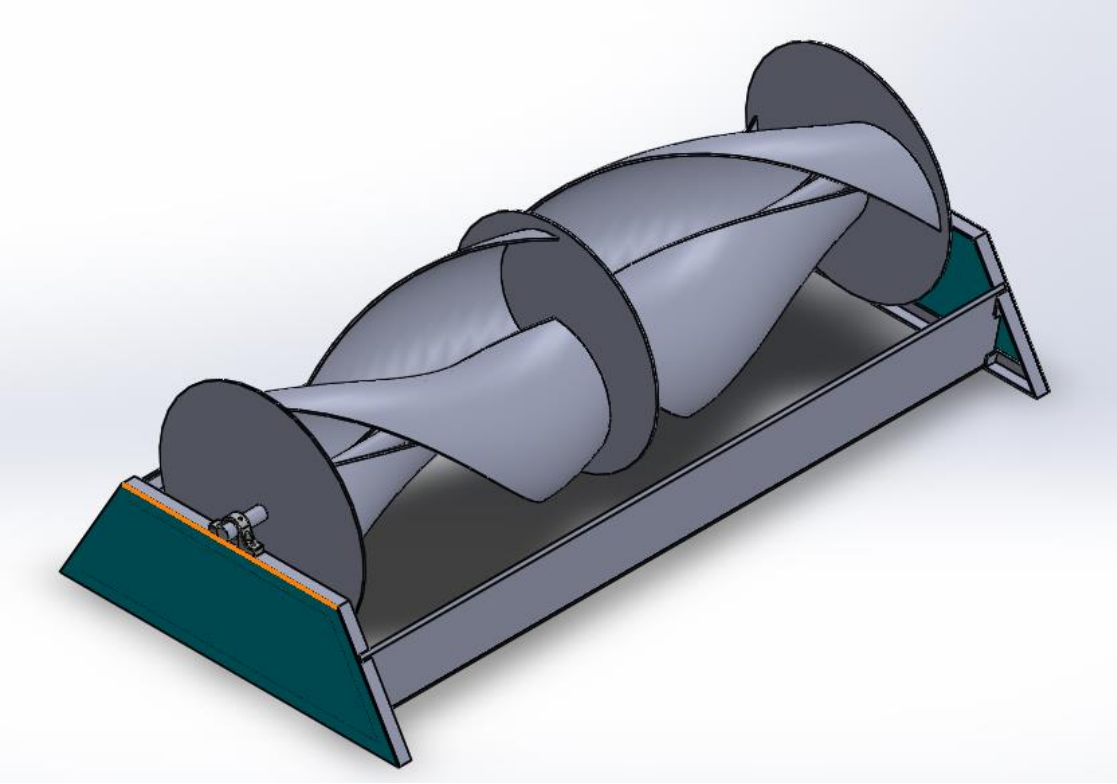


Figure 6: Turbine Assembly

CHAPTER 2: LITERATURE REVIEW

As discussed before, hydropower generation is the greatest source of electricity today. A lot of work has been done towards it. Different kinds of turbines have been developed to achieve this objective. There are some conventional turbines such as Pelton, Kaplan and Francis Turbines and some Hydrokinetic Turbines. Hydrokinetic turbines are popular for their economic feasibility for real-world utilizations and commercialization. As explained in previous chapter in background, turbines are generally classified into two categories, axial flow and cross flow turbines, based on rotor axis orientation. Axial flow turbines have rotor axes parallel to the water flow and are propeller-type rotors. On the other hand, cross flow turbines have rotor axes vertical to water plane (vertical axis) and horizontal to water surface (in-plane axis). Cross flow turbines can be further divided into two categories of design; Darrieus design type turbine and Savonius design type turbine. Water interaction with the blades in Darrieus type rotor develops a force, known as lifting force, which acts as a driving force. For Savonius type rotors, driving force is generated by the drag force [1]. Here is study of different parameters governing the design of Vertical Axis Turbines as found in literature;

2.1 GENERAL LIFT AND DRAG FORCES

Lift force is caused by pressure and viscous effects from the air that is exerted on an airfoil. It acts orthogonally to the relative velocity and is oriented perpendicular to the drag force. The air exerts a force on the airfoil in the direction of the flow called drag, which is caused by pressure and

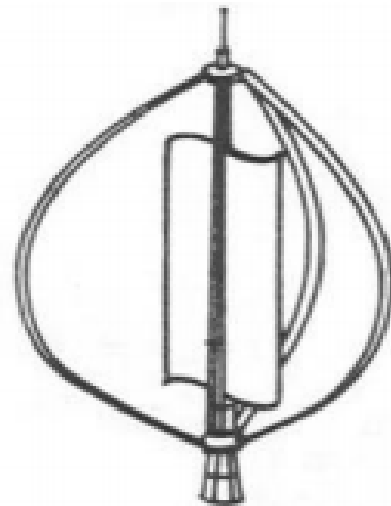


Figure 7: Darrieus and Savonius combination turbine
(D.Anderson, 2007)

friction. The normal and tangential forces are found by summing the tangential and normal components of the lift and drag forces. The AOA i.e. Angle Of Attack is defined as being the angle between the relative velocity and the chord, shown in figure below. The chord is the straight line from the leading edge to the trailing edge of the wing profile. For objects which are designed to generate lift, the contribution from the viscous effect can be neglected, so the lift force is only depending on the pressure differences at the airfoil's surfaces. The drag force is a sum of friction (skin) drag and pressure (form) drag. The induced drag which is related to end effects of airfoils will be described separately. Both lift and drag coefficients are dependent the airfoil's orientation in the flow. This orientation is represented by the AOA. Airfoils are designed to generate lift and minimize drag. [32]

2.1.1 Lift Force

Lift is mainly generated by the pressure distribution on the surface of an airfoil. This pressure distribution is formed by the shape of the airfoil. The airfoil is designed so that the top and bottom surfaces can have different curvatures, which means that the flow moving over and under the airfoil will have to take a different length path. For a symmetrical profile, this difference is created by changing the AOA.

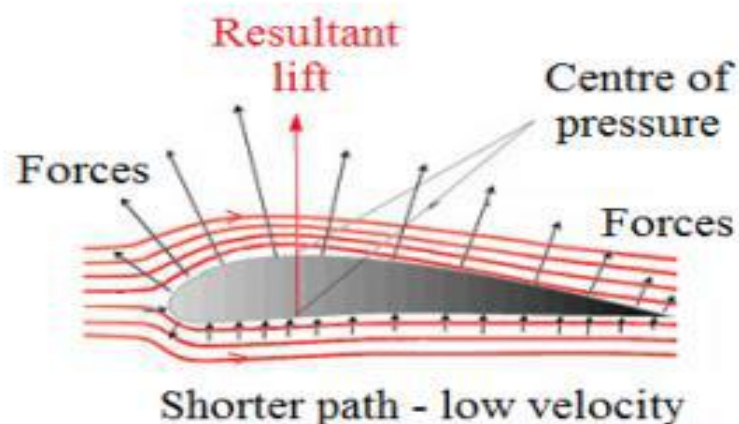


Figure 8: Pressure Distribution on an Airfoil (ManWell, 2002)

Conservation of mass requires that the amount of air before and after the airfoil must remain constant. The difference in path length causes the flow over the longer section (the top surface) to briefly accelerate. According to Bernoulli's equation this increase in velocity results in a decrease in pressure. The pressure vacuum along the top surface of the airfoil creates a pressure gradient which is what creates the lift force. The pressure distribution on an airfoil can be seen in figure below. [3]

As the flow passes over the airfoil the faster moving fluid on the top must begin to decelerate as it approaches the trailing edge. The flow at the trailing edge must have the same velocity on the top and the bottom of the airfoil. If it does not then there will be a shearing in the flow that will cause significant amount of drag and turbulence downstream of the airfoil. If the flow does have the same velocity on top and bottom of the profile and the trailing edge is sharp, then the Kutta Condition will be met. This will result in a stagnation point at the trailing edge which allows the air to be smoothly shed from the airfoil. Figure below shows how there initially is a large pressure drop on the top surface due to the acceleration of the flow, but as the flow passes over the profile the pressure drop decreases so that the velocities on both surfaces of the trailing edge are equal.

$$C_L = \frac{F_L}{\frac{1}{2}\rho V^2 A} \quad (1)$$

The lift coefficient is a non-dimensional number that describes how effectively an airfoil changes the flow to generate lift. Due to the different geometries of airfoils, there are unique values of the coefficients of lift for each airfoil. These lift coefficients is plotted based on AOA at a given Reynolds number.

2.1.2 Drag force

Drag forces resist the forward motion of an object, so for vehicles such as airplanes the drag force must be compensated by an increase in thrust. Drag is broken into two categories: friction (skin) drag and pressure (form) drag. Frictional drag is due to surface shear stresses and is a function of viscosity. The Reynolds number is inversely proportional to viscosity, so at higher Reynolds numbers the contribution from frictional drag will become less significant. When frictional drag is exerted on a body in a turbulent flow it is also a function of the surface roughness. A smooth and nonporous material has less frictional drag than a rough or porous one.

The pressure drag is a function of the frontal area and the pressure difference between the front and back of an object. The pressure drag is small for streamlined objects such as an airfoil. When it is not possible for the flow to follow the surface, it separates from a location called the separation point. The flow after the separation point can be described as highly turbulent and creates eddies that are in a low pressure region. This means that the pressure drag will continue to increase as the AOA increases because the pressure gradient from leading to trailing edge is increasing.

Drag is calculated with an equation very similar to lift. Like lift, a non-dimensional number, called the coefficient of drag, has been created to express the drag as a function of AOA and Reynolds number. [9]

$$C_D = \frac{F_D}{\frac{1}{2}\rho V^2 A} \quad (2)$$

Considering finite wings, the end effect of the wings will be an important parameter, because there will be a fluid leakage between the top and bottom of the airfoil. The leakage on a

lift producing wing is caused by the flow curling from the high pressure side, to the low pressure side.

The curling of flow around the wing tips creates trailing vortex at both wing tips, as shown below. These tip vortices tend to take the surrounding air with them, which creates a small downwards velocity also called downwash.

2.2 COMPARISON BETWEEN VERTICAL AND HORIZONTAL AXIS TURBINES

After a detailed comparison of various types of hydrokinetic turbines, Guney and Kaygusuz [2] conclude that vertical axis turbines are more suitable for limited water flow rate streams. They also state that horizontal axis turbines are more efficient and are able to self-start. Axial flow turbines are mainly used in ocean due to their higher efficiency.

Khan et al. [3] reported in his paper that cylindrical rotor shape has a real advantage over the disk rotor shape of axial flow turbines. In his other paper [4], Khan et al. deduces that vertical axis turbines are simpler in design, but inherently not self-starting. Table below shows the comparison between horizontal axis and vertical axis turbines;

Table 1: Comparison between Axial flow and Cross flow turbines

| S. No | Attributes | Axial flow/horizontal axis | Cross flow/vertical axis turbine |
|-------|--------------------------|----------------------------|----------------------------------|
| 1 | Efficiency | High | Lower |
| 2 | Self-Starting Capability | Yes | Inability |

| | | | |
|---|--|---|--|
| 3 | Manufacturing cost, transportation cost & maintenance cost | High | Lower |
| 4 | Shape of rotor | Disc type | Cylindrical shape |
| 5 | Airfoil shape | Yes | Doesn't need |
| 6 | Blade size | Large | Configured with smaller and simpler blade |
| 7 | Problems in river stream | Clogged with debris found in rivers | Can deflect incoming debris [5] |
| 8 | Other requirements | Requirements for water sealed components (generator, gearing, and bearing, etc.) | No |
| 9 | Installation ability | Only as single unit due to disc-shaped rotor and impossible to deploy in small, narrow river. | Deploy as a single unit in small rivers and stacked together to deploy in bigger rivers. |

Cross flow turbines have advantages such as small size blades, less manufacturing cost, less transportation cost, and less maintenance cost which makes them suitable for free flow applications to extract the energy from river, etc.

As stated before, vertical axis turbines have two general designs; Derrius and Savonius. Derrius turbine blades are straight bladed, Gorlov turbine blades are of helical structure and have same working principle as Derrius turbine while Savonius turbine blades are of helical or straight

structure. Savonius hydrokinetic turbine is simple in design and easy to fabricate at lower cost. However, they still lack popularity when compared to horizontal axis turbines.

2.3 SAVONIUS HYDROKINETIC TRUBINE

Savonius rotor is an ‘S’ type rotor made up of two semi-circular blades with a small overlap between them as shown in Fig 2. With better starting characteristics, Savonius rotor has the ability to accept fluid from any direction. However, it has low aerodynamic efficiency as compared to that of Derrieus rotor. As mentioned before, Savonius rotor is a drag type rotor. Water applies drag force on both advancing and returning blade. The difference in magnitudes of the forces acting on advancing and returning blades acts as the driving force. Kamoji MA [6] deduces that advancing blade with concave side facing the water experiences more drag force than the returning blade. This is because the drag coefficient for concave surface is more than that of convex surface.

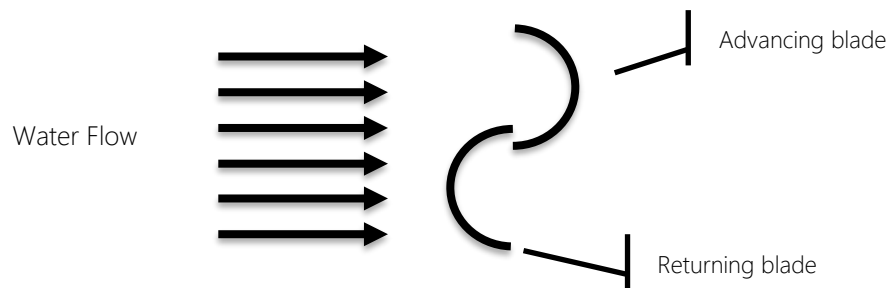


Figure 9: Basic shape of Savonius Rotor

In above figure, ‘H’ is the representation of the height of rotor whereas diameter of the rotor is denoted by ‘D’. The ratio between these two dimensional quantities i.e. ‘H’ and ‘D’ is coined as ‘The aspect ratio’. There is another parameter upon which the performance of Savonius rotor depends and it is called as ‘the overlap ratio’ (β) which is normally expressed in the form of $\beta = \frac{e}{d}$, where ‘e’ is the overlap and ‘d’ is the diameter of the blade. Upon impingement of the free force the advancing blade creates a drag force while the returning blade develops a returning force

from the outflow through the gap (overlap) that is in opposing direction creating a pair of couple forces of which we get the generated torque and power.

There are similarities between the Savonius hydrokinetic turbine and the Savonius wind rotor systems regarding the physical principles upon which their operations work to generate optimal energy. But as water's density is 835 times more than the air so Savonius hydrokinetic turbines are able to extract more energy even at lower water speeds [7]. Savonius

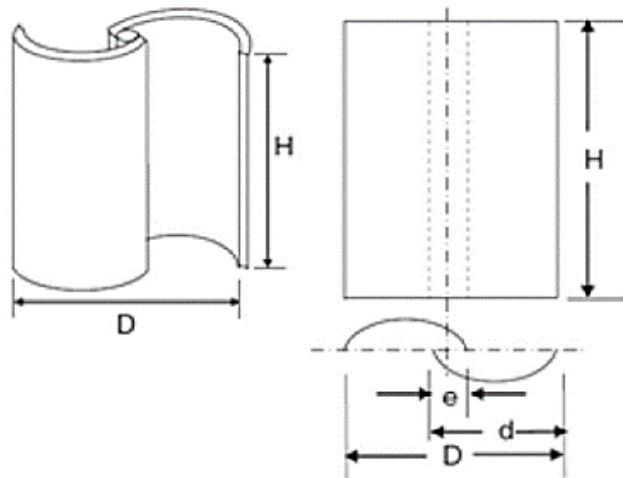


Figure 11: A typical two-bladed Savonius rotor

hydrokinetic turbines can be made operational in conditions where water velocity is as low as 0.5

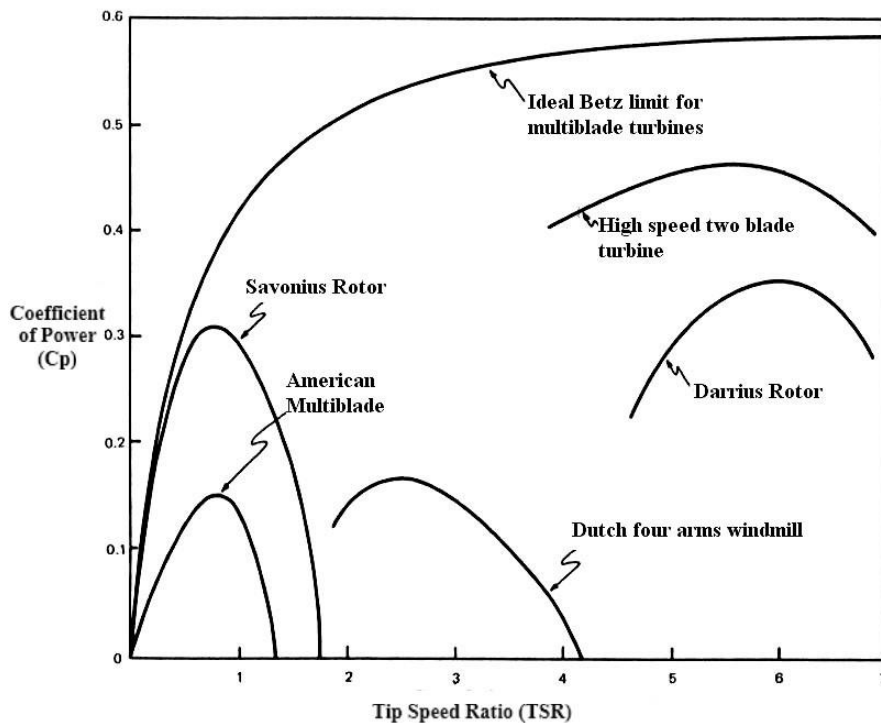


Figure 10: Betz Limits

m/s and above [8-9]. Published results of different researchers have clearly indicated that Savonius rotor performance is affected by different geometric, operational and flow parameters. Working range of savonius rotor. can be seen clearly from betz limit.

2.4 DESIGN PARAMETERS



2.4.1 Aspect Ratio

Aspect ratio (AR) plays a decisive role to obtain satisfactory performance of turbine which can be defined as the ratio of turbine height, H and its diameter D. Aspect ratio is one of the major players to get satisfactory performance of the turbine. Its definition shows us that it is the ratio of turbine height 'H' and its diameter 'D'. Studying the effect of aspect ratio, Alexander and Holownia [10] conducted a number of wind tunnel tests on different Savonius geometries with different wind speeds ranging from 6 to 9 m/s with the conclusion that those turbines which have higher aspect ratios are poised to perform better. The operational similarity between wind turbine and the hydro turbine enables us to perform the experimentation using air as the fluid as a water counterpart with the attained results best fit for both. Zhao et al. [11] considering helical Savonius

rotor conducted its numerical analysis to improve its efficiency. Following table shows the results from different researchers.

Table 2: C_p Results with different Aspect Ratios

| SR. no | Methodology | Turbine Tested | Aspect Ratio | Optimum Value | Optimum Performance Value (C_p) | Additional Parameters |
|--------|--------------|--|---------------------|---------------|--|--|
| 1 | Experimental | Two bladed Semi circular | 1.2-4.8 | 4.8 | $C_p = 0.243$ | With end plate and flat shield |
| 2 | Numerical | Two bladed helical (180°) Savonius Rotor | 1-7 | 6 | $C_p = 0.2$ | Overlap ratio = 0.3 |
| 3 | Experimental | Modified Savonius rotor without shaft | 0.6-1.0 | 0.7 | $C_p = 0.21$ $C_t = 0.3$ At Re = 150,000 | Overlap ratio = 0, Blade arc angle = 12.4°, blade shape factor (p/q) of 0.2 and end plate parameter (D_0/D) of 1.1 |
| 4 | Experimental | Helical Savonius rotor with a twist of 90° | 0.88, 0.91 and 1.17 | 0.88 | $C_p = 0.105$ Re = 120,000 | Overlap ratio = 0 |
| 5 | Experimental | Two bladed semi circular | 0.5-5.0 | 5.0 | $C_p = 0.14$ | Overlap = 0, Single Stage |

There are a number of studies for the wind as well as for water as working fluid which reveal that aspect ratio ranging from 1.0 to 2.0 also exhibits good performance of Savonius rotors [12-15]

2.4.2 End Plate

From the studies of several researches it is concluded that performance of the turbine improves significantly by using end plates [16-18]. End plates prevent the fluid leakage from the concave side of the blades to the external flow thus keeping the pressure difference between the concave and the convex sides of the blades at satisfactory levels [16]. Jeon et al. [19] observed the performance of helical Savonius wind turbines (twist angle 180 degree). End plate area ratio (ER)

is the ratio of the area of the end plate (AE), and cross-sectional area of turbine perpendicular to the rotating axis i.e. $AC (\frac{1}{4} \pi d^2)$. Four different shapes of end plate with four end plate area ratio (ER=0 to 1), as shown in figure 5 were taken into consideration for the study.

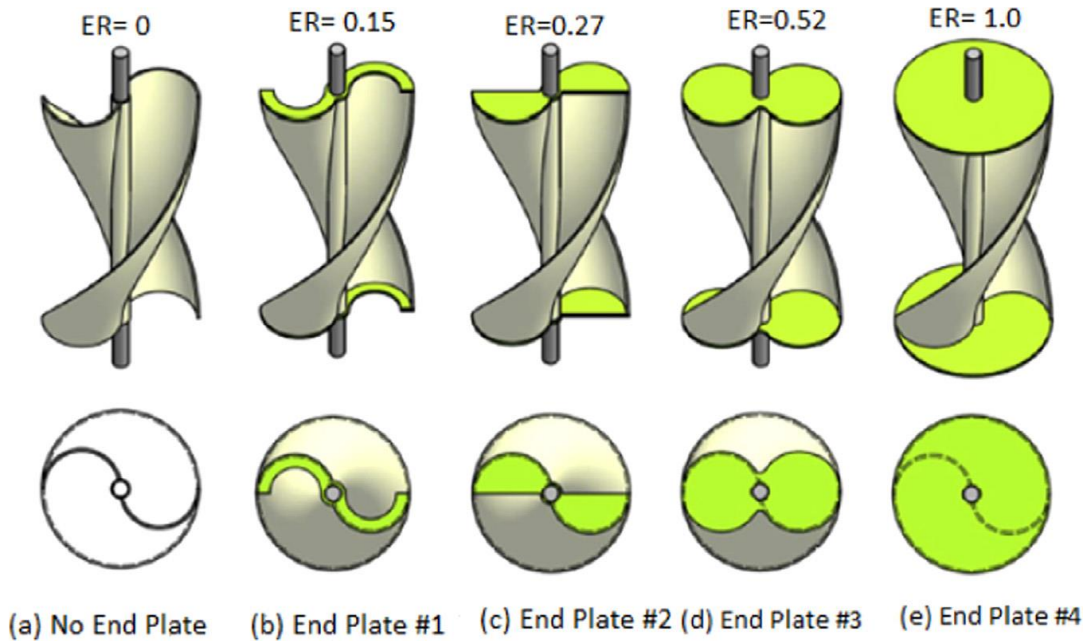


Figure 13: Helical Savonius rotors with various shapes and sizes of end plates

The study concluded that circular end plate (ER=1) is the best choice for maximizing power and torque coefficients for helical Savonius wind turbines. Figure 6 presents power coefficient of the helical Savonius wind turbines with end plates of various shapes

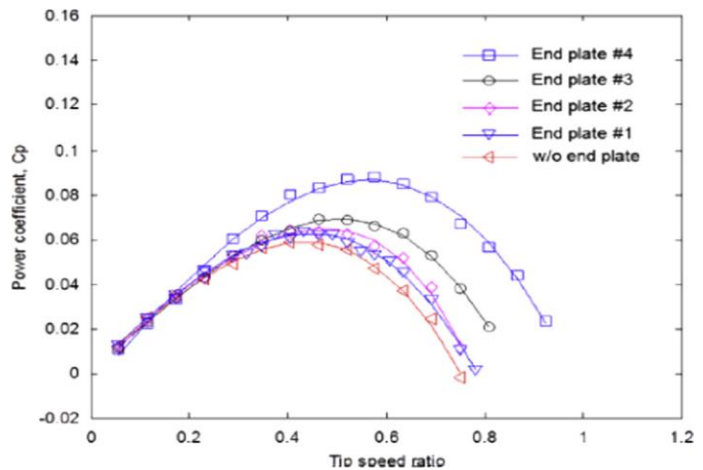


Figure 12: Power coefficient of helical savonius wind turbines with end plates of various shapes and size

and sizes and reveals that the larger area of end plate, the higher the power coefficient is obtained.

Several researchers show that the optimum performance for any given turbine was obtained at the end plate diameter = 1.1D (D = rotor diameter)

2.4.3 Overlap Ratio

Overlap ratio is the ratio of blades overlapped length to the diameter of a blade. In order to optimize the performance of Savonius rotor, Overlap ratio plays a critical role. A number of

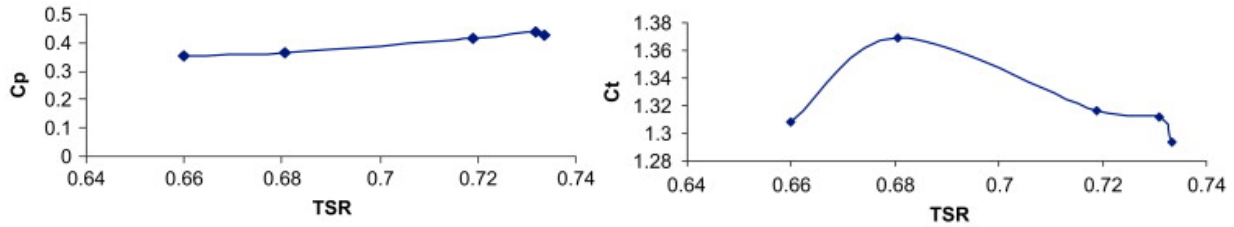
| S. No. | Methodology | Turbine tested | Range used | Optimized value of overlap ratio | Coefficient of performance | Additional parameters used in study |
|---|--|--|--|--|---|---|
| 1. | Experimental | Two Bladed Semi Circular | -0.07, 0.2, 0.22 | 0.22 | $C_p=0.147$ | Aspect ratio=2.4, Gap ratio=0.07 |
| 2 | Numerical | Two Bladed Helical (180°) Savonius rotor | 0.0-0.5 | 0.3 | 0.181 | Aspect ratio=2.0 |
| 3 | Experimental | Modified Savonius rotor without shaft | 0.0, 0.10 and 0.16 | 0.0 | 0.17 | Blade shape factor (p/q)=0.2, aspect ratio of (H/D)=0.77, blade arc angle (ψ)=124° |
| 4 | Experimental | Helical Savonius rotor with a twist of 90° | 0.0-0.16 | 0.0 (Rotor without shaft) | $C_{pmax}=0.165$ at TSR=0.8 and Re=120,000; $C_{pmax}=0.175$ at TSR=0.9 and | Aspect ratio for rotor with shaft=1.0; Aspect ratio for rotor without |
| <i>Table 3: Effect of Overlap Ratio</i> | | | | | | |
| 6 | Experimental | 2 bladed Savonius turbine | 0.0-0.3 | 0.3 | $C_p=0.327$ at Re=588,300 | Aspect ratio =2.0 |
| 7 | Experimental and numerical | 2 bladed Savonius turbine | 0.0-0.45 | 0.2 | $C_p=0.254$ at Re=1.5 × 10 ⁵ | Aspect ratio=1.875 and Semicircular blade |
| 8 | Two-dimensional unsteady numerical study | 2 bladed Savonius turbine | 0.0-0.30 | 0.2 | $C_{T5}=0.224$ at U=10.44 m/s | Aspect ratio=1.0 |
| 9 | Experimental | 3 bladed Savonius rotor and Combined rotor (3 bladed Savonius-3 bladed Darrieus rotor) | 0.0-0.20 | Overlap ratio=0.20 and 0.0 for simple Savonius rotor and Combined rotor respectively | For simple Savonius turbine, $C_{pmax}=0.46$ and for combined rotor $C_{pmax}=0.51$ | Aspect ratio of Savonius rotor = 2.5 and 1.25 for 3 bladed Savonius rotor and Combined rotor respectively |
| 10 | Experimental | 2 bladed Savonius turbine with flat and round blade edges | 0.1-0.7 for flat edge; 0.1-0.5 for round edge | 0.50 for flat edges and round edges | $C_{T5} \approx 0.485$ at Re=120,000 | Aspect ratio =1.0 for both flat and round edges |
| 11 | Experimental | 2 bladed Savonius turbine having single and two stage | 0.0-0.333 | 0.167 for single stage and 0.333 for two stage | $C_p=0.173$ for single stage $C_p=0.144827$ for two stage rotor at 0° phase shift at velocity (U)=8 m/s $C_p=0.267$ at TSR= 1.0 | Aspect ratio for single stage and double stage = 1.088 and 2.176 respectively |
| 12 | Experimental under field condition | 2 bladed Savonius turbine | 1/8-7/8 | 1/4 | | Aspect ratio=1.52 |
| 13 | Experimental | 2 bladed Savonius turbine | 0.0-0.5 | 0.15 | Not reported | Aspect ratio =1.0, U=6 m/s |
| 14 | Numerical | Savonius-turbine model based on double stacking design | 0.1-0.6 | 0.21 | Average Torque (Tm)=0.1362 at velocity=0.169 m/s | Aspect ratio=2.0 |
| 15 | Numerical | Double stepped Savonius rotor with two paddles and two end-plates | 0.1-0.5 | 0.242 | $C_{T5} = 0.33$ at Re=1.56 × 10 ⁵ | Aspect ratio=2.0 |

studies to determine the optimum value of overlap ratio were carried out in the available literature. Effect of overlap ratio on the performance of Savonius rotor through various investigations is given in the following table;

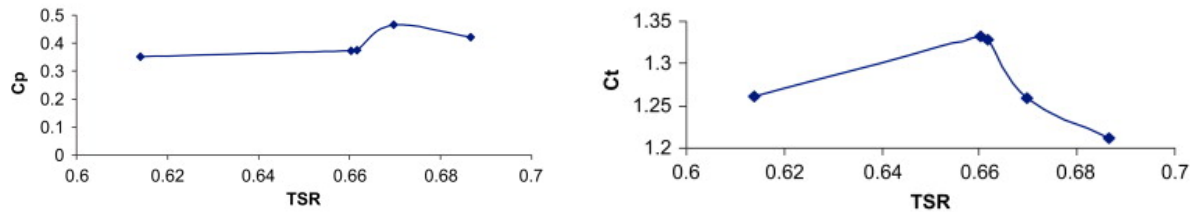
The results given in the literature for different overlap ratios are given bellow;

- Simple three bladed Turbine:

Overlap ratio = 0

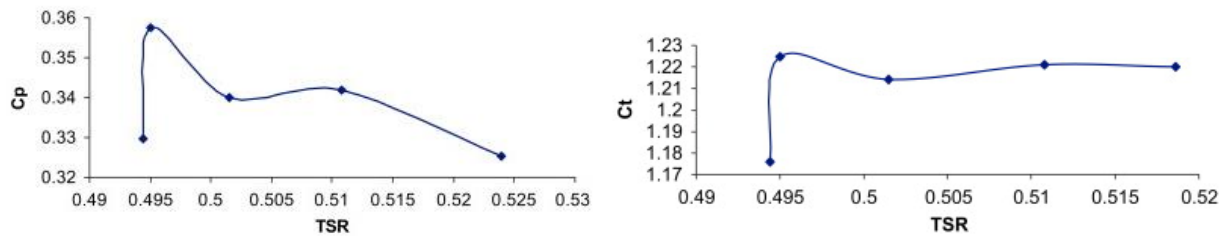


Overlap ratio = 0.162



Overlap ratio = 0.2

It can be observed at no overlap ratio condition that both C_p and C_t increase with increase in TSR but afterwards both start decreasing. The maximum power coefficient is 0.3579 at a tip-speed ratio of 0.4950 and the maximum torque coefficient is 1.2246 at the same tip-speed ratio. At 16.2% overlap, again both C_p and C_t increase with TSR and then decrease. A maximum C_p of 0.4380 at TSR 0.7320 and the maximum C_t of 1.3693 at TSR 0.6806 are obtained. Figures show the variations of power and torque coefficients, respectively, for a three-bucket Savonius rotor at 20% overlap, which follow the same trend as at previous conditions and maximum power coefficient is



0.4668 at a tip-speed ratio of 0.6696 and the maximum torque coefficient is 1.3318 at the TSR of 0.6603 are obtained. Thus it is clear that there

is definite improvement of power coefficient with the increase in overlap. Further, the torque coefficient has also marginally improved with increase in overlap [34][35].

2.4.4 Number of blades

The number of blades plays a critical role in the performance of Savonius turbine depending upon the operating conditions. With the increase of the blades number, fluctuations of the dynamic and static moment of a Savonius rotor, along the angular positions of the advancing bucket, can be reduced. Following table shows a summary of studies carried out for number of blades;

Table 4: No. of blades vs C_p

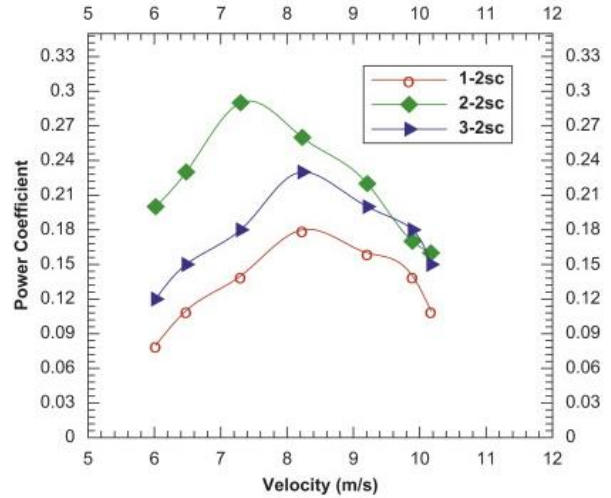
| S. no | Methodology | Turbine Tested | Range used | Optimum number of blades | Optimum Performance Value | Additional Parameters |
|-------|--------------|---|------------|--------------------------|---|------------------------------------|
| 1 | Numerical | Single stage Helical (180°) Savonius rotor | 2 & 3 | 2 | $C_p = 0.165$ | A/R = 2 & Overlap = 0 |
| 2 | Experimental | Semicircular savonius rotor | 2, 3 & 4 | 2 | $C_p = 0.09$ | Single stage, A/R = 0.5 No overlap |
| 3 | Experimental | Single, two, three stage savonius rotor having semicircular and twisted blade shape | 2 & 3 | 2 and twisted | $C_p = 0.19$ at $U = 8.23$ m/s $C_p = 0.31$ at $U = 7.3$ m/s $C_p = 0.24$ at $U = 8.23$ m/s | A/R = 1.58 |
| 4 | Experimental | Single stage Savonius rotor | 2 & 3 | 2 | $C_p = 0.24$ at $Re = 864,000$ | Overlap ratio = 0.15, A/R = 1.0 |
| 5 | 2D-CFD | Single stage Savonius rotor | 2 & 6 | 6 | $C_p = 0.3$ at $U = 3$ /s | A/R = 2.0 |

In order to observe the effect of number of blade, Saha et al. (S.R. no. 3) carried out an experimental investigation on Savonius rotor with a twisted and semicircular rotor having single, two and three stages. It is observed when the number of blades is increased to three, the fluid which focuses on one blade, gets reflected back on the following blade so that the following blade rotates in the negative direction as compared to the succeeding blade. It is therefore, with an increase of

number of blades, the rotor performance decreases. It can be concluded from the experimental evidence that a two-bladed system gives optimum performance. The study resulted in maximum CP of 0.31 for two bladed twisted Savonius rotor having two stages. Following are the graphical results:

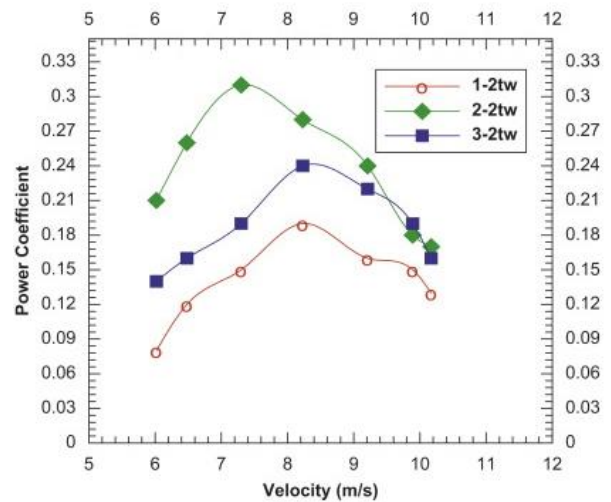
This graph shows power coefficient for the three cases;

1. 2sc: Single stage two bladed semi circular
2. 2sc: Two stage two bladed semi circular
3. 2sc: Three stage two bladed semi circular

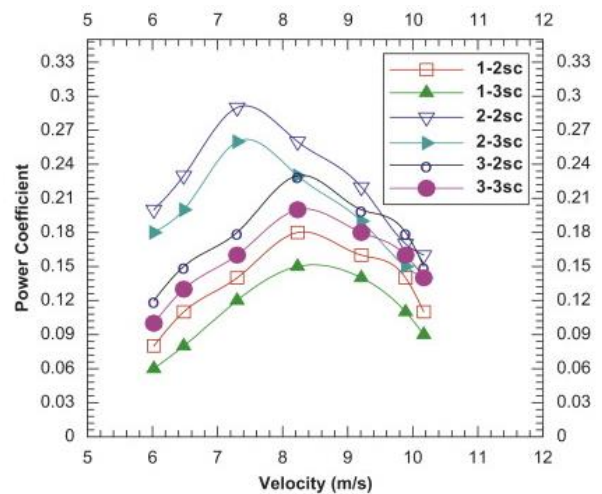


This graph also shows the power coefficients for three different turbines:

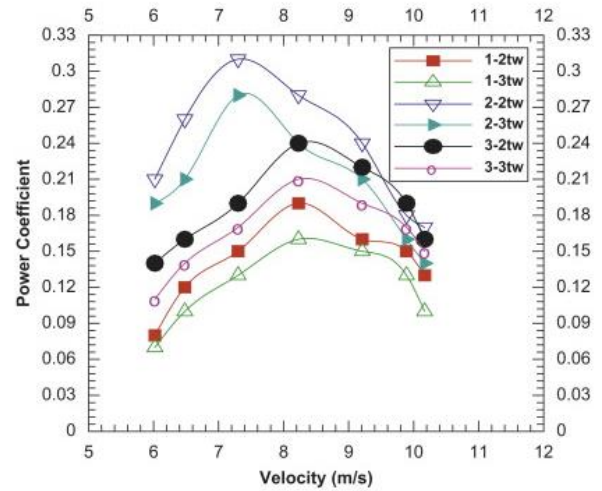
1. 2tw: Single stage two bladed twisted
2. 2tw: Two stage two bladed twisted
3. 2tw: Three stage two bladed twisted



Following graph shows Variation of power coefficient with velocity for semicircular Savonius rotor system. It can be seen in the graph that the maximum performance is shown by the turbine with two stage and two blades.



Following graph shows Variation of power coefficient with velocity for twisted Savonius rotor system. Graph shows that turbine having two stage and two blades shows the best performance;



Mahmoud et al. [20] studied experimentally the performance of single and double stages Savonius wind turbine with zero overlap ratio to determine an optimum number of blades. It was reported that the two blades rotor offers better performance than three and four blades rotors for all aspect ratios as well as for single or double stages too. Sheldahl et al. [27] reported that the power coefficient for two blades and three blades is found to be optimum at TSR of 0.9 and 0.7, respectively. Fig. 9 illustrates the effect of TSR on power coefficient of two and three-bladed rotors;

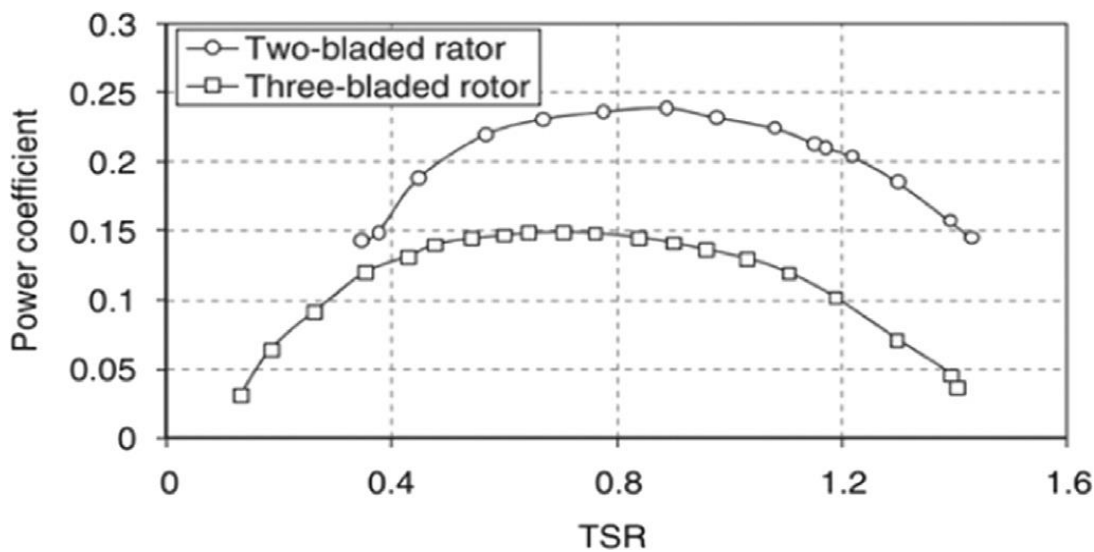


Figure 14: Variation of power coefficient with respect to TSR for two and three bladed rotor

2.4.5 Multi Staging

Due to large static torque variation with rotor angle, the performance of single stage rotor is affected adversely. Stacking of single stage rotors one above the other with a phase shift is expected to smoothen the coefficient of static torque variations and produce a positive coefficient of static torque at all the rotor angles in a cycle of 360° . This stacking of single stage rotors one above the other is called as multi-staging. In two stages, one single stage rotor is placed over another single stage with a 90° phase shift. In three stages, the three single stage rotors are placed one above the other with a phase shift of 60° to one another. A standard Savonius rotor would be unable to start on its own because of its very low starting torque. In order to improve starting torque characteristics, numbers of stages are increased by several researchers. Following table shows some of the results:

Table 5: Stages vs C_p

| S. R no | Methodology | Turbine Tested | Range used | Optimum number of blades | Optimum Performance Value | Variation of static torque |
|---------|--------------|---|------------|--------------------------|---|--|
| 1 | Experimental | 2 bladed savonius rotor | 1-3 stages | 1 | $C_p = 0.157$ at $Re = 80,000$ for single stage and $A/R = 1.0$ | Minimum for three stage and maximum for single stage |
| 2 | Experimental | 2 bladed semi circular savonius rotor | 1 and 2 | 2 | $C_{TS} = 0.38$ at wind velocity = 10 m/s | - |
| 3 | Experimental | Savonius turbine having semicircular and twisted (12.5°) shape | 1-3 stages | 2 | $C_p = 0.31$ for twisted and 0.29 for semicircular at $U = 7.3$ m/s | - |

From the table it can be derived that a turbine having **2 stages and twisted blades is optimum for minimizing variation in torque and maintaining high power coefficient**. Three stage shows the

minimum variation in torque but due to increase in inertia power coefficient decreases. Therefore, two stage rotors are optimum to use.

In order to investigate the effect of number of stages at different Reynolds numbers, Kamoji et al. [21] studied the performance of single stage, two stage Savonius rotor and three stage Savonius rotor. For the same rotor aspect ratio of 1.0, by increasing the number of stages (stage aspect ratio decreases), the performance was decreased. Authors also reported that three stage rotors offer lower variation in coefficient of static torque as compared to that of two stages or single stage rotor, as shown in Fig. 7. Two stages Savonius rotor gives higher specific power (W/m²) than single stage rotor. Similarly, double stages rotor has higher static torque and consequently higher static torque coefficient compared to the single stage rotor.

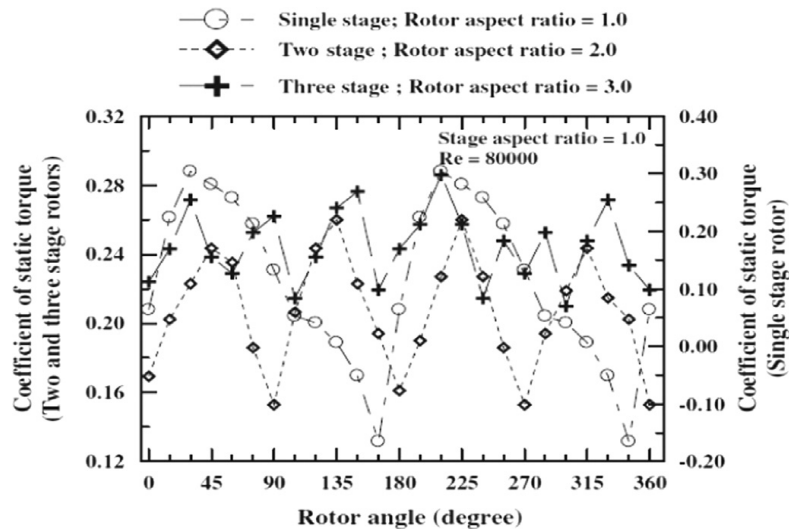


Figure 15: Comparison between two and three stage rotors for static torque coefficient

2.4.6 Deflector Plate

Many researchers have adopted various techniques to maximize the performance and improve the starting torque characteristics of Savonius turbine with wind as working medium. These include use of guide vanes, V-plate deflector, deflector plate, deflector plate and blade with flat and circular shielding. Best deflector position. And geometrical parameters can be calculated using following table [41].

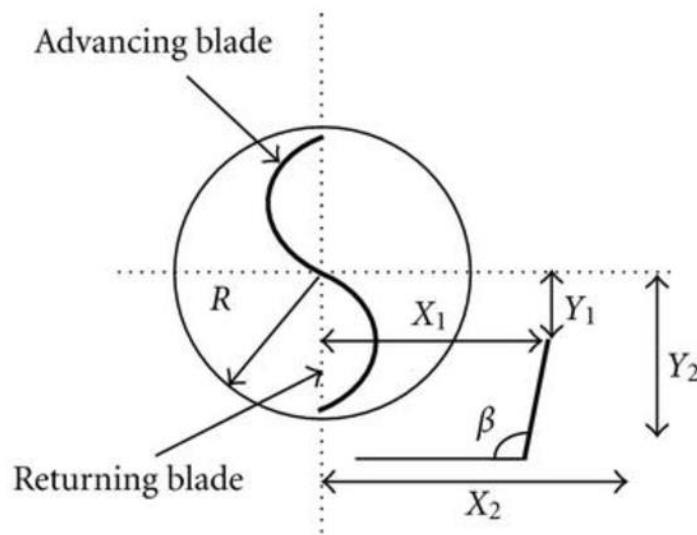


Figure 16: Schematic of modified Savonius rotor with space parameters of deflector plate

Following is the demonstration of different parameters used in this table [41];

Table 6: Geometric parameters for deflector plate positioning

| Configuration No. | $\frac{x_1}{R}$ | X_1 (mm) | $\frac{x_2}{R}$ | X_2 (mm) | $\frac{y_1}{R}$ | Y_1 (mm) | β |
|-------------------|-----------------|------------|-----------------|------------|-----------------|------------|-------------|
| 1 | 1.102 | 135 | 1.102 | 135 | 0.450 | 55 | 90° |
| 2 | 1.240 | 152 | 1.102 | 135 | 0.450 | 55 | 101° |
| 3 | 1.877 | 230 | 1.102 | 135 | 0.450 | 55 | 137° |
| 4 | 1.102 | 135 | 1.877 | 230 | 0.450 | 55 | 44° |
| 5 | 1.877 | 230 | 1.102 | 135 | 0.882 | 108 | 159° |
| 6 | 1.877 | 230 | 1.102 | 135 | 0 | 0 | 123° |
| 7 | 1.102 | 135 | 1.877 | 230 | 0 | 0 | 58° |
| 8 | 1.102 | 135 | 1.102 | 135 | 0 | 0 | 90° |

2.4.7 Rotor Angle

Various studies suggest that the highest static torque value lies in the range of $\theta = 30\text{--}60^\circ$. Kianifar and Anbarsooz [22] reported torque variation with respect to rotor angles and concluded that torque increases with increasing wind speed and its maximum values appear near the angle of 60° and its minimum values appear near the angle of 120° for all test rotors.

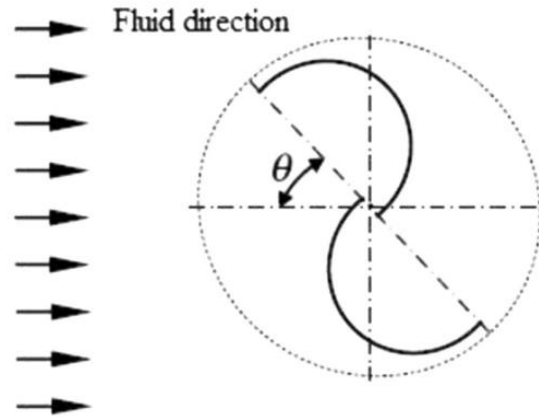


Figure 17: Representation of rotor angle

2.4.8 Reynold Number

Reynolds number is the most important parameter which defines the fluid flow characteristics around a Savonius rotor. Many researchers studied the effect of Reynolds number on the performance of savonius rotor that show that greater the Reynolds number greater will be the output parameters. Kamoji et al. [24] investigated the influence of Reynolds number for a modified Savonius rotor (without shaft) for an overlap ratio of zero, aspect ratio of 0.7, blade arc angle of 124° , and blade shape factor of 0.2. They reported that with the increase in the Reynolds number, CP increases. As a result, the coefficient of power was found to be increased by 19% as Reynolds number increases from 80,000 to 150,000. It was also observed that coefficient of static torque with rotor angle is almost independent of the Reynolds number in the range of 80,000 to 150,000. Kamoji et al. [25] and Hayashi et al. [26] also stated that coefficient of power increases with increase in the Reynolds number for conventional single, two and three stage Savonius rotors.

2.4.9 Tip Speed Ratio (TSR)

TSR always remains as a matter of interest to the researchers since the beginning of research on the Savonius rotor. The mechanical construction of turbine i.e. number of blades and rotor diameter are the key factors which affect the optimal TSR. If the rotor buckets spin too slowly, buckets will not be capable of capturing most of the water and a less amount of water will pass through the rotor. Nevertheless, if the rotor buckets spin too fast, then it will always travel through used turbulent water. There must be sufficient time lapses between two buckets traveling through the same location so that nearby water can move in and power can be harnessed from it, not the used, turbulent water. The graphical representation of the effect of TSR on the performance has been shown in the “Effect of Overlap Ratio”.

2.4.10 Installation Parameter

Nakajima, in his paper, explains the effect of installation parameters on power performance of a turbine. Following are the installation parameters he focused on in his paper:

- The distance between the rotor and the bottom wall
- The distance between the rotor and the water surface
- The rotation direction of the rotor

In addition, he examined flow patterns around the rotor associated with power performance. He plotted several graphs for performance against the clearance ratio (Clearance ratio (H_C/D_R) is a dimensionless parameter which defines the distance between a rotor and a bottom wall of the channel with respect to rotor diameter.

Results indicated that the maximum coefficient of power is 0.26 for clearance ratio of 0.73 for counterclockwise (CCW) direction of rotation. For CCW, the maximum power coefficient is found to be better at clearance ratio less than 0.73, while for clockwise (CW) direction of rotation the maximum power coefficient is on the higher side at clearance ratio greater than 0.73

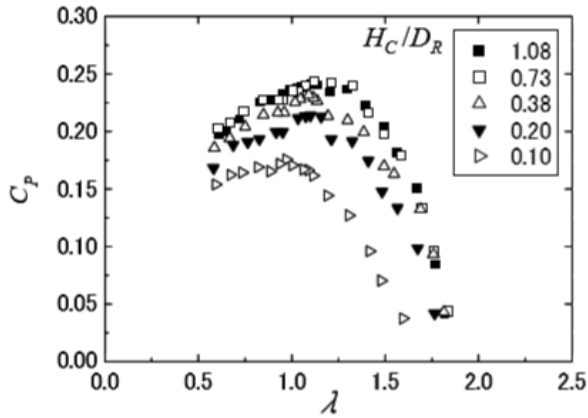


Figure 20: Performance for CW

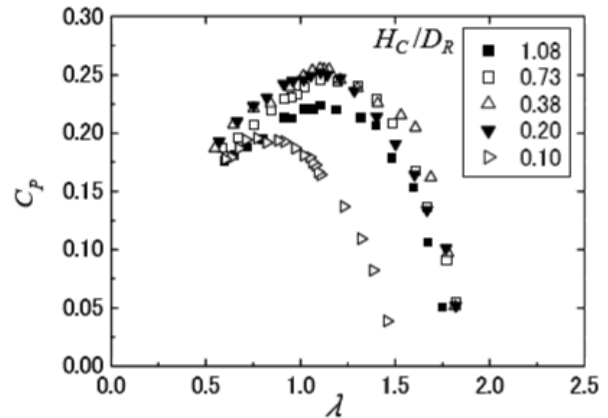


Figure 18: Performance for CCW

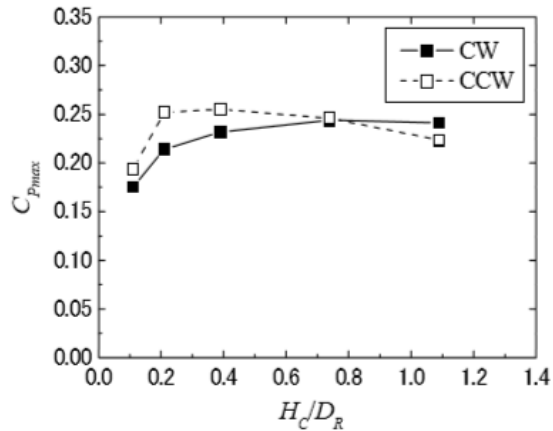


Figure 19: Max Power Coefficient vs Clearance Ratio

CHAPTER 3: METHODOLOGY

3.1 DESIGN

3.1.1 Dimensions

Theoretical dimensions are calculated from the betz limit which is 0.593 and power usage of a normal house which we take as 18 kWh. Dimensions are scaled down for the prototype and following are the prototype dimensions.

3.1.1.1 Rotor Dimensions

Length(One-Stage) = L or H = .75 m

Rotor Dia = D = 0.4747 m

Shaft Dia = e' = 0.04 m

$$D = 2d - e \quad \text{----- i}$$

$$(e - e')/d = 0.242 \quad \text{---- ii}$$

Solving above 2 equations;

Blade dia = d = 0.2927759 m

Overlap (including shaft dia) = e = 0.1108518 m

Rotor center to center of blade distance = $d/2 - e/2 = 0.0909205$

Sheet Thickness = 5mm

3.1.1.2 Deflector plate position

$$X1/R = 1.24 \Rightarrow X1 = .3237454 \text{ m}$$

$$X2/R = 1.102 \Rightarrow X2 = .28771567 \text{ m}$$

$$Y1/R = .450 \Rightarrow Y1 = .11748825 \text{ m}$$

$$Y2/R = 1.177 \Rightarrow Y2 = .307297045 \text{ m}$$

For Deflector-Dimensions [42]

3.1.2 2-D Drawings

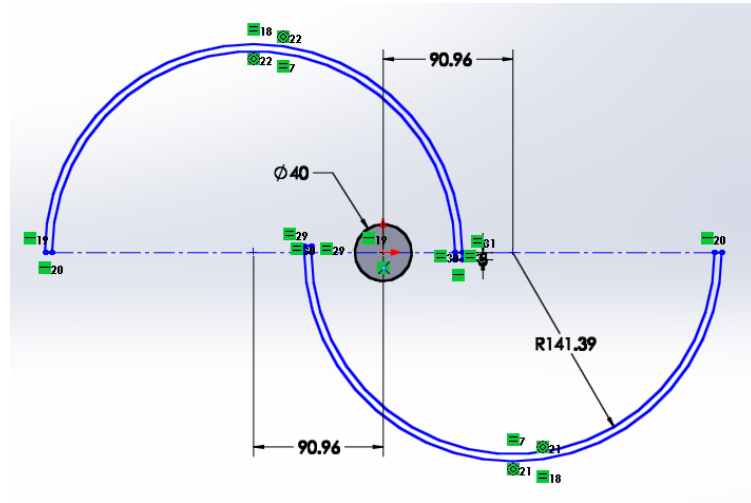


Figure 21: 2D Sketch of Rotor

3.1.3 3-D Model of Rotor

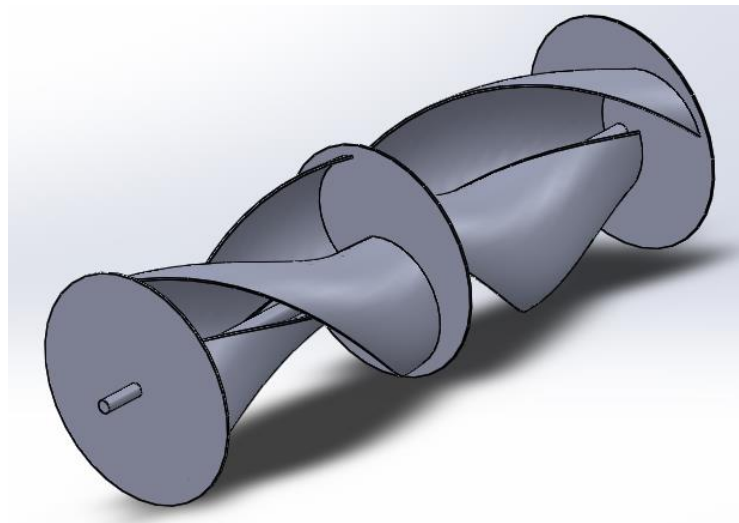


Figure 22: 2 Stage - Helical Rotor

3.1.4 Bearing Housing

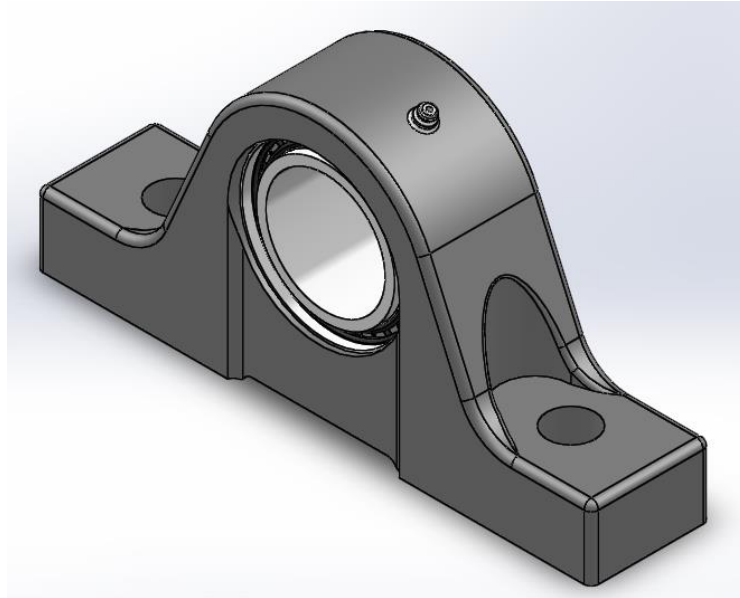


Figure 23: Bearing Housing

3.1.5 Frame Assembly

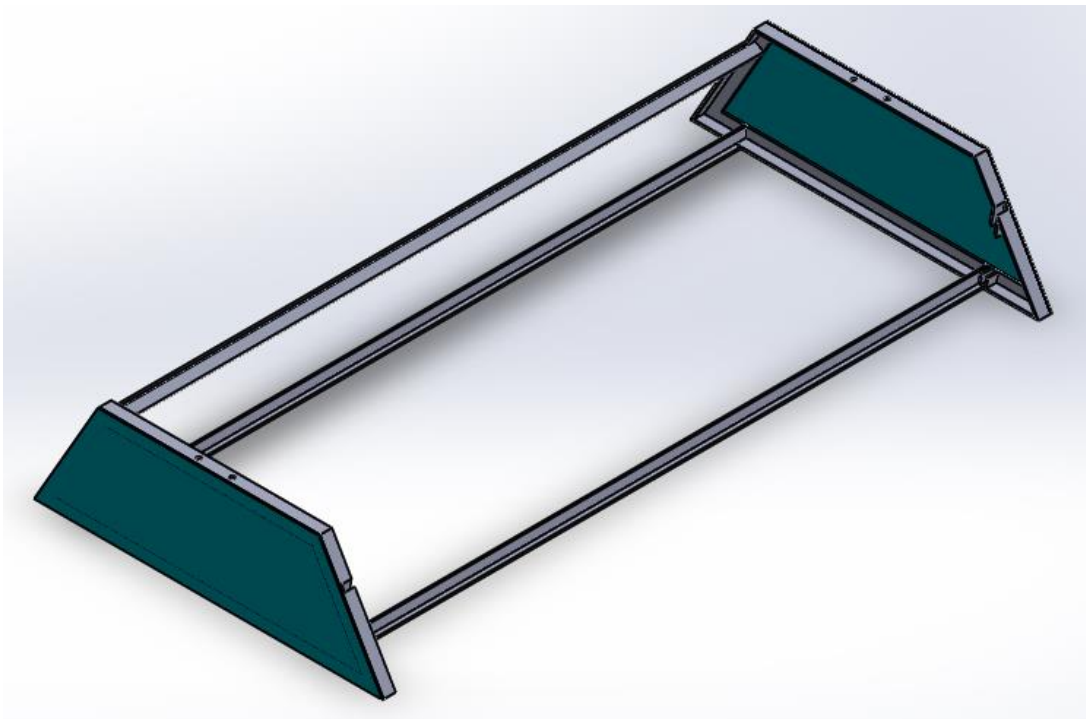


Figure 24: Frame Assembly

3.1.6 Assembly

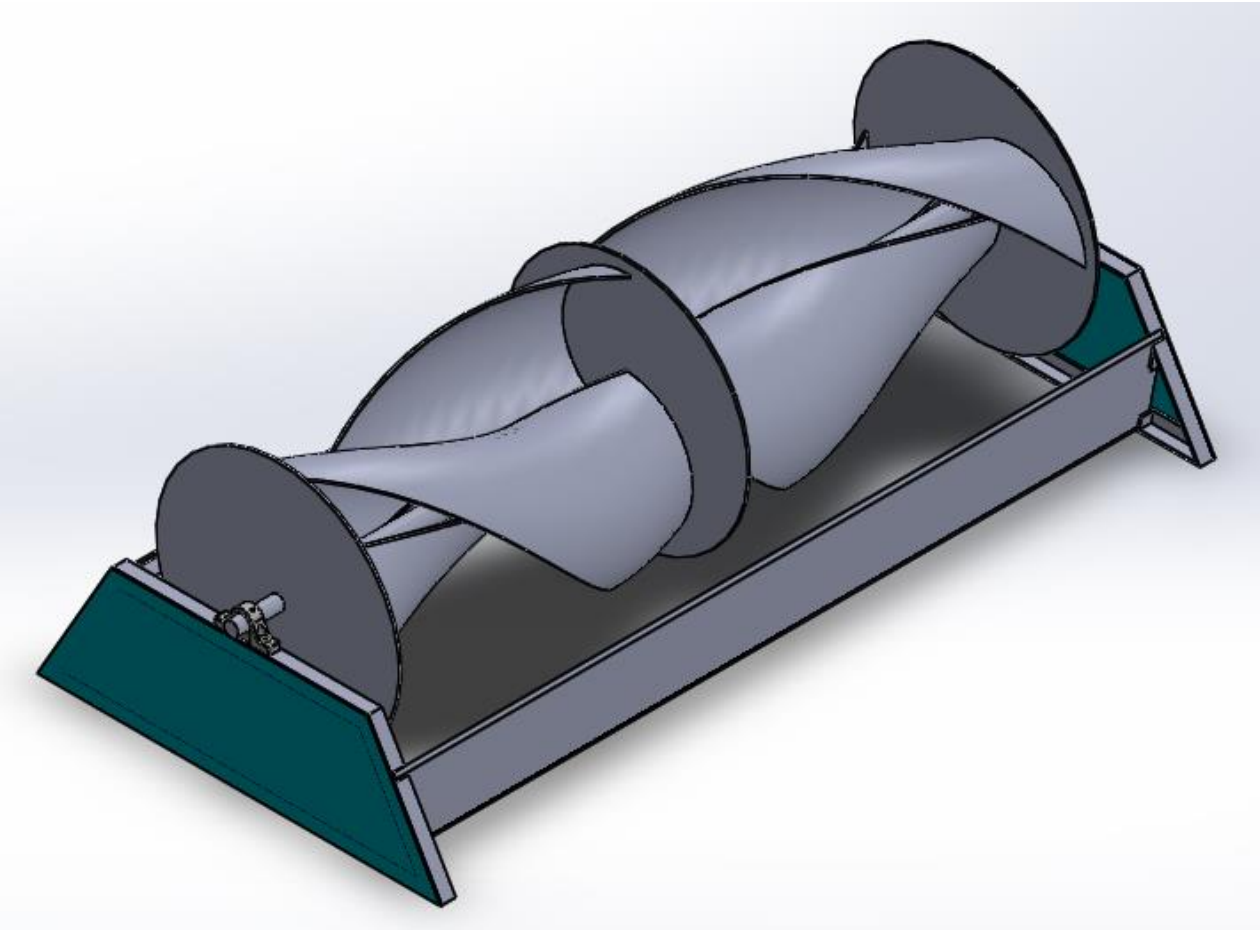


Figure 25: 3D Assembly of Turbine

3.2 MATHEMATICAL MODEL

The working principle of Savonius rotor is based on the difference of drag force between the advancing and the returning blades. This difference in drag forces creates torque in the rotor which results in the performance of the turbine.

3.2.1 Coefficient of Power

Coefficient of power of a Savonius turbine is given by:

$$C_p = \frac{P}{P_A}$$

It can also be written as:

$$C_p = \lambda \times C_t$$

3.2.2 Power Available

Power available in the water is given by:

$$P_A = \frac{1}{2} \rho A_S V^3$$

3.2.3 Power Generated

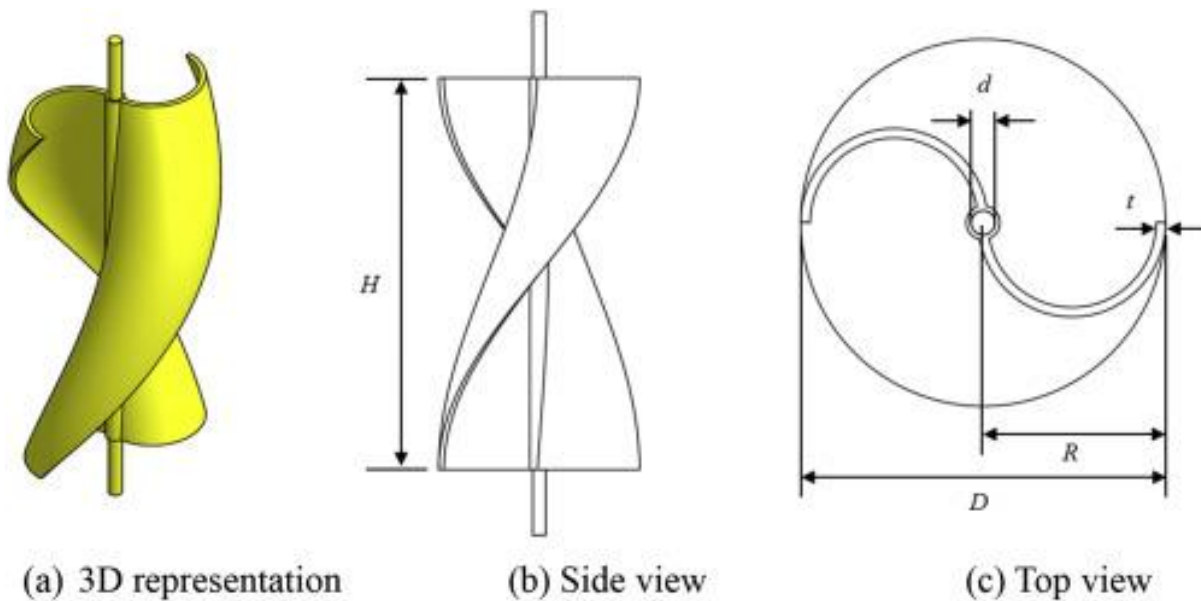
Power generated by the savonius rotor is determined by:

$$P = T \times \omega$$

3.2.4 Swept Area

As the rotor turns, its blades generate an imaginary surface whose projection on a vertical plane to wind direction is called the swept area. The amount of energy produced by a wind turbine primarily depends on the rotor area, also referred to as cross-sectional area, swept area, or intercept area. The swept area for Savonius wind turbine can be calculated from the dimensions of the rotor:

$$\text{Swept Area} = A_s = H \times D$$



3.2.5 Tip Speed Ratio (TSR)

The tip speed ratio is the ratio of the product of blade radius and angular speed of the rotor to the wind velocity. The tip peripheral velocity of the rotor (V_{rotor}) is defined as:

$$V_{rotor} = \omega \times \frac{D}{2}$$

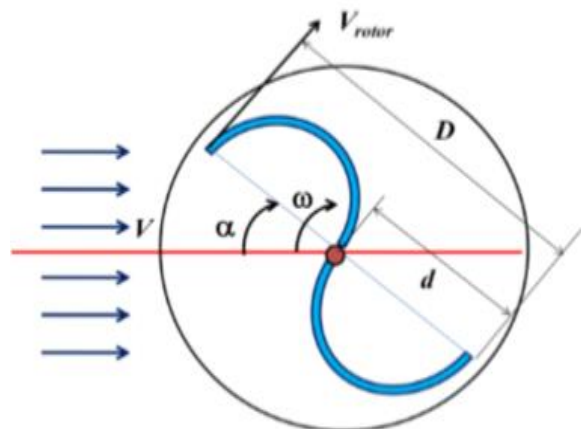


Figure 26: Scheme of a Savonius rotor showing the tip velocity of the rotor

Now the Tip Speed Ratio (TSR) of a turbine is expressed as:

$$\text{The Tip Speed Ratio} = \text{TSR} = \lambda = \frac{V_{\text{rotor}}}{V} = \frac{\omega \times D/2}{V}$$

3.2.6 Torque Coefficient (C_t)

It is defined as the ratio between the actual torque developed by the rotor (T) and the theoretical torque available in the wind (T_w), thus the torque coefficient (C_t) is given by:

$$C_t = \frac{T}{T_A}$$

3.2.7 Torque Available

Torque available is the maximum torque that can be produced in ideal case. It is defined as:

$$T_A = \frac{1}{4} \rho A_s D V^2$$

3.2.8 Required Torque

Torque produced by rotor is defined as:

$$T = \frac{F_A D}{2} \int_0^{\pi/2} \cos \theta \sin(\theta + \phi) d\theta$$

3.2.9 Force Available

$$F_A = \frac{1}{2} \rho A_s V^2 C_d$$

3.3 Flow SIMULATION

Ansys FLUENT is used to perform 2-dimensional CFD analysis of the rotor. The dimensions are deduced using the maximum power required for a house and the Betz Limit. The dimensions of the rotor are then scaled down for prototyping.

A 2D design of three different rotors are developed in Ansys Design Modeler. Models with deflector, without deflector and without overlap.

A fine mesh, as shown below, is generated to deduce accurate results. Graphs of C_p are to be deduced against different TSR (0.1 – 1.4) and constant Reynolds Number. Water inlet velocity is set at 1 m/s. The flow is transient and k-epsilon model is used. The difference in the drag coefficients of returning and advancing blades causes a generation of force on the advancing blade. The product of this force and rotor radius generates a torque. Therefore, values of C_t are written in a file and are later used to calculate C_p using the relation mentioned above.

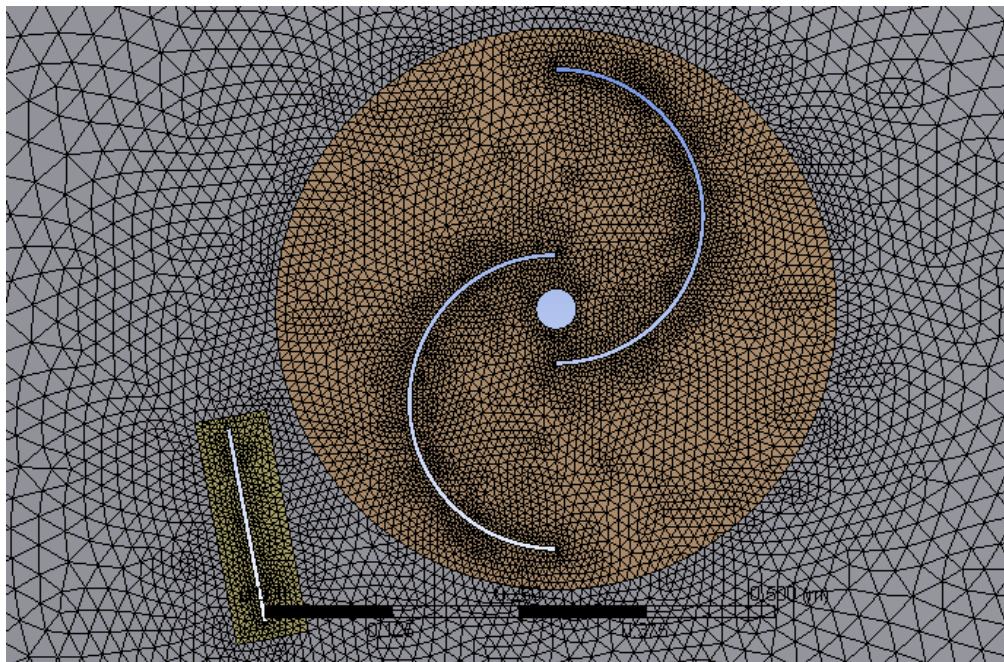


Figure 27: Mesh generated in Ansys

CHAPTER 4: RESULTS and DISCUSSIONS

4.1 THEORETICAL

Three different simulations are run for three different geometries of turbine. This is done to select the best model for the turbine. Three geometries of turbines are:

1. Savonius turbine with zero overlap
2. Savonius turbine with an overlap ratio of 0.242
3. Savonius turbine with a deflected plate and an overlap ratio of 0.242

Torque coefficient graphs for each case are plotted against rotor angle. Fig below shows Ct curve of the turbine with respect to different rotor angles. Maximum Ct occurs when the rotor is at angle of almost 210 degrees. This is when the returning blade becomes the advancing blade with the angle of 30 degrees. The curve also shows that negative torque is also generated. This effects on the average torque produced by the rotor at a specific TSR and Reynolds Number.

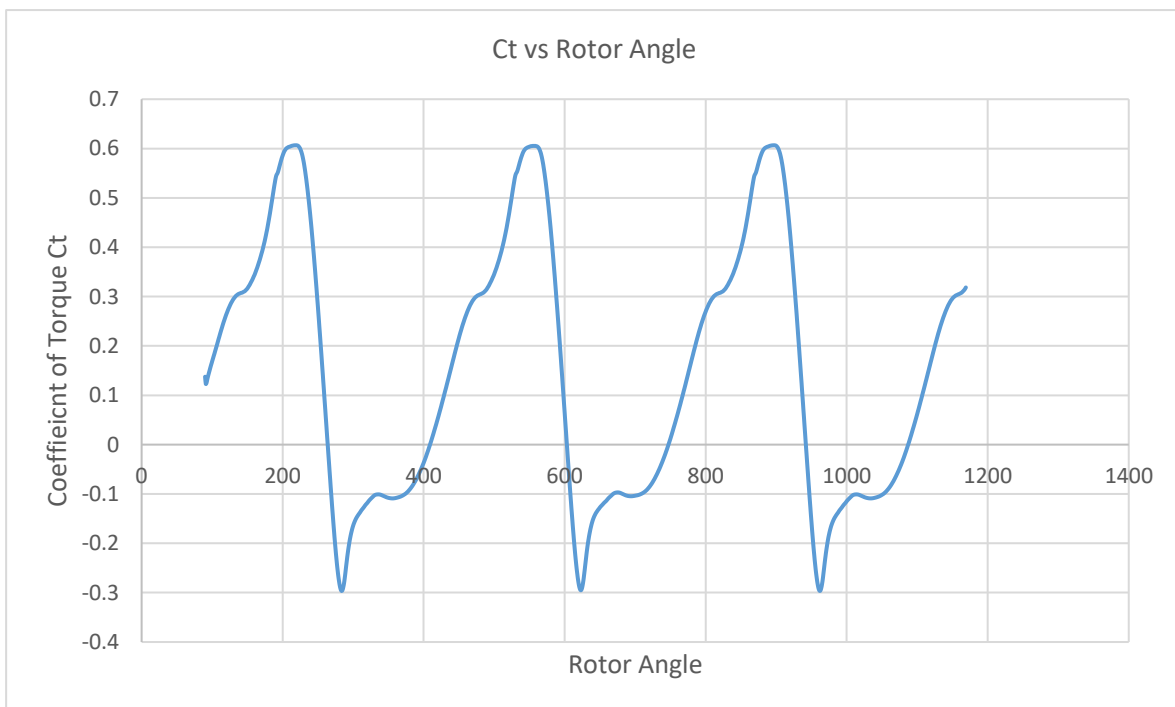


Figure 28: Savonius Turbine with zero Overlap

Fig below shows the effect of overlap ratio on the C_t curve. The graph shows that the maximum C_t is reduced from 0.61 to 0.53. However, it also shows that the negative torque effect has been phased out with the addition of overlap ratio. Addition of overlap reduces the resultant force acting on the returning blade which increases the overall resultant force acting on the rotor. This increases the average torque produced by a Turbine at a specific TSR and Reynolds Number. The maximum torque produced is again at the angle of approximately 210 degrees which, as mentioned before, is the point when returning blade is the advancing blade with 30 degrees of rotor angle.

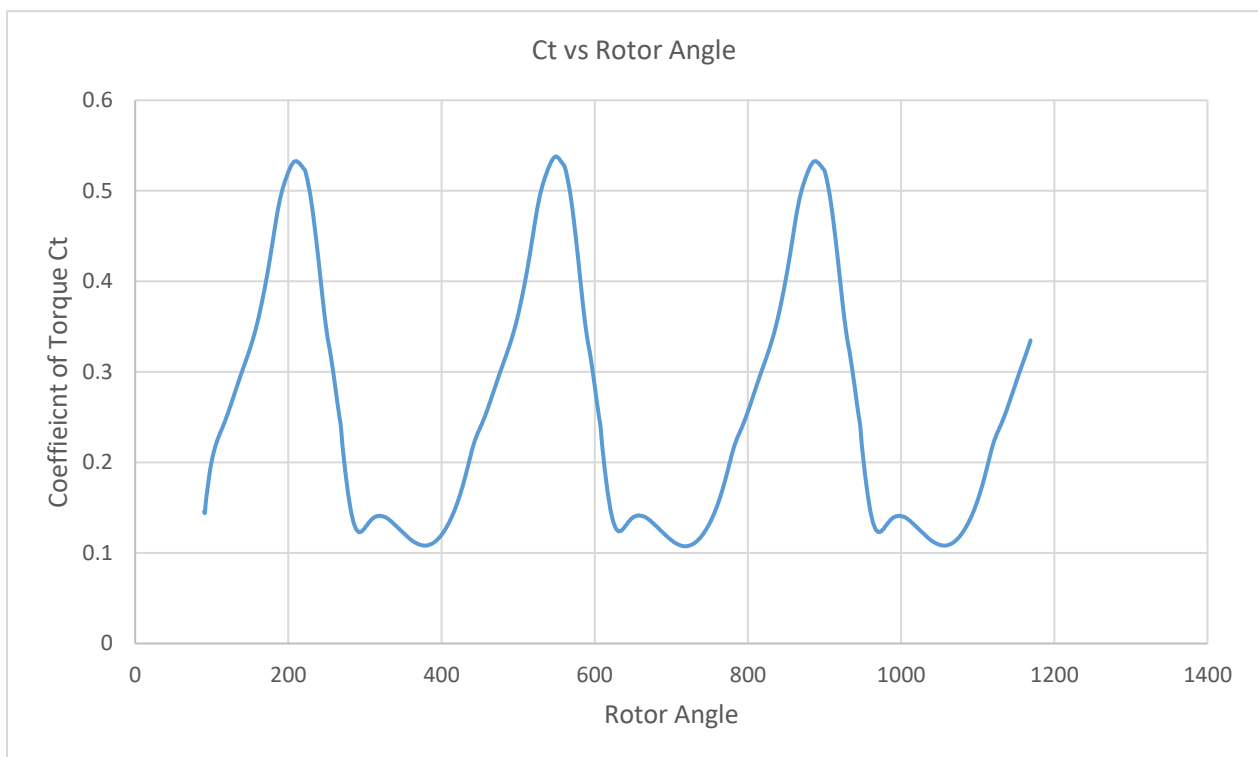


Figure 29: Savonius Turbine with an overlap ratio of 0.242

The problem of maximum torque reduction in previous design is compensated in our third design. The addition of deflector increases both the maximum coefficient of torque back to approximately 0.61. It also increases the minimum coefficient of torque. Deflector deflects the incoming flow towards the returning blade resulting in the decrease of the force acting on it. This

increases the overall resulting coefficient of torque. The maximum C_t acts at an angle of 200 degrees i.e. when returning blade acts as an advancing blade with an angle of 20 degrees.

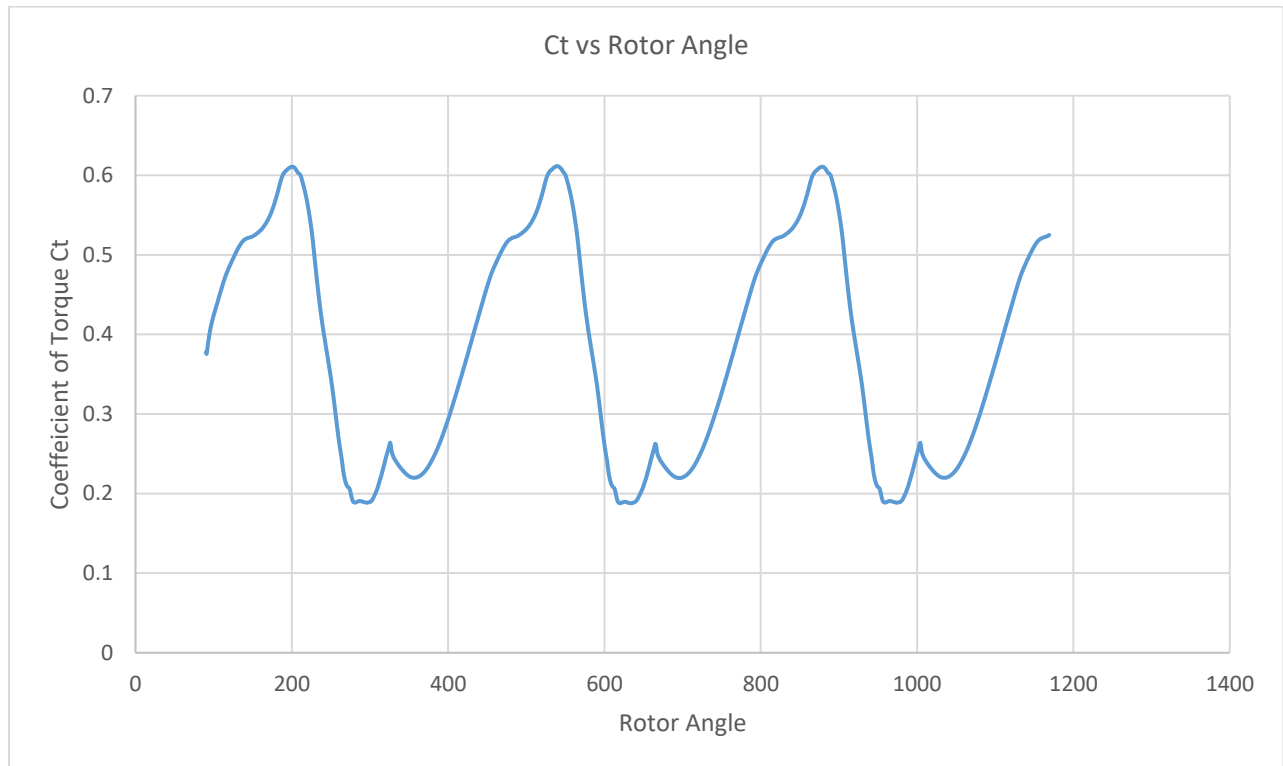


Figure 30: Savonius Turbine with deflector and overlap ratio of 0.242

Coefficient of performance is calculated using the following formula:

$$C_p = TSR \times C_t$$

For every TSR (0.1 to 1.4), average C_t is deduced and C_p is calculated. This is done for all of the three cases. The effect of overlap ratio is shown in the Fig 2a. Maximum C_p of 0.154 for the turbine with no overlap ratio occurs at $TSR = 0.6$. C_p in this case also reduces to negative values which is not a desired result. For the turbine with overlap, maximum C_p of 0.26 occurs at $TSR = 0.9$. This C_p curve shows that the blade overlap increases the performance of the savonius turbine.

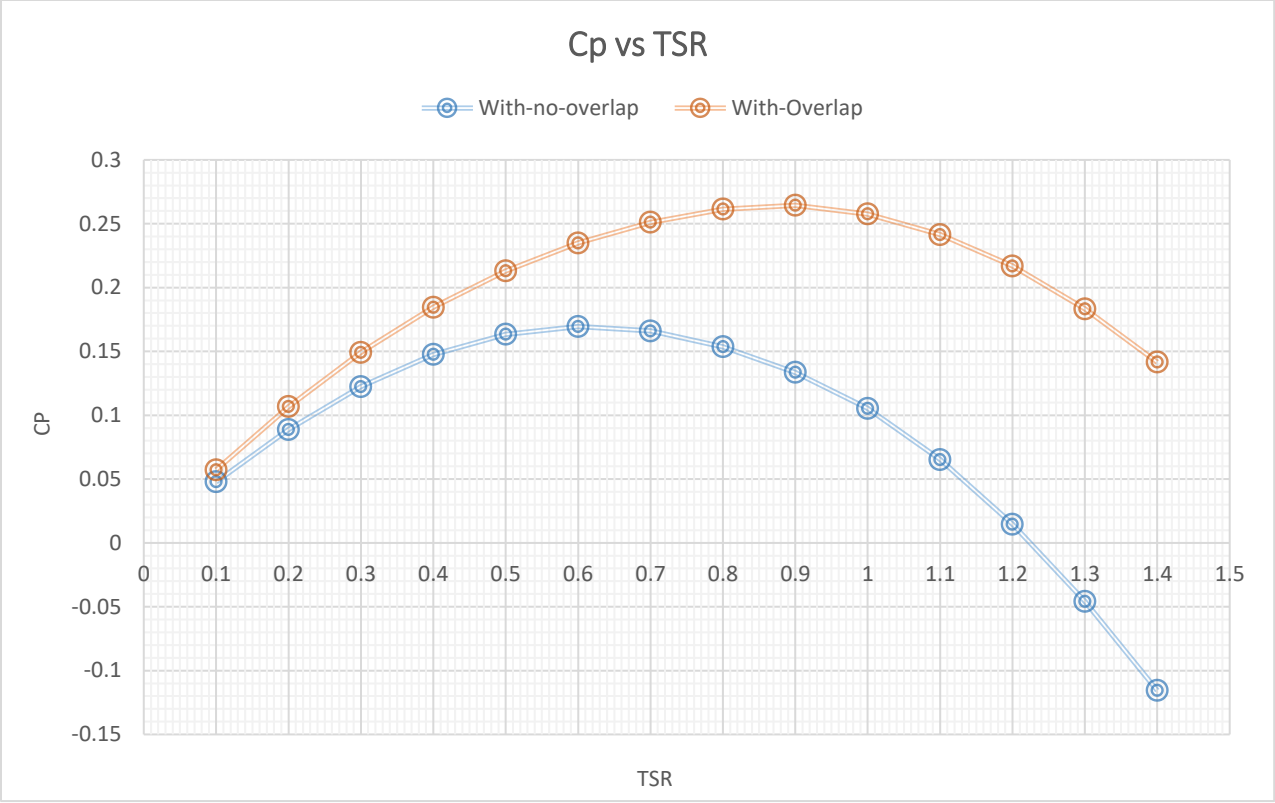


Figure 31: Effect of Overlap Ratio

As mentioned before, the effect of deflector increases the performance of the turbine. This is proved by the curve shown below in Fig below. The addition of deflector increases the maximum C_p to 0.34. This value of maximum C_p also occurs at $TSR = 0.9$.

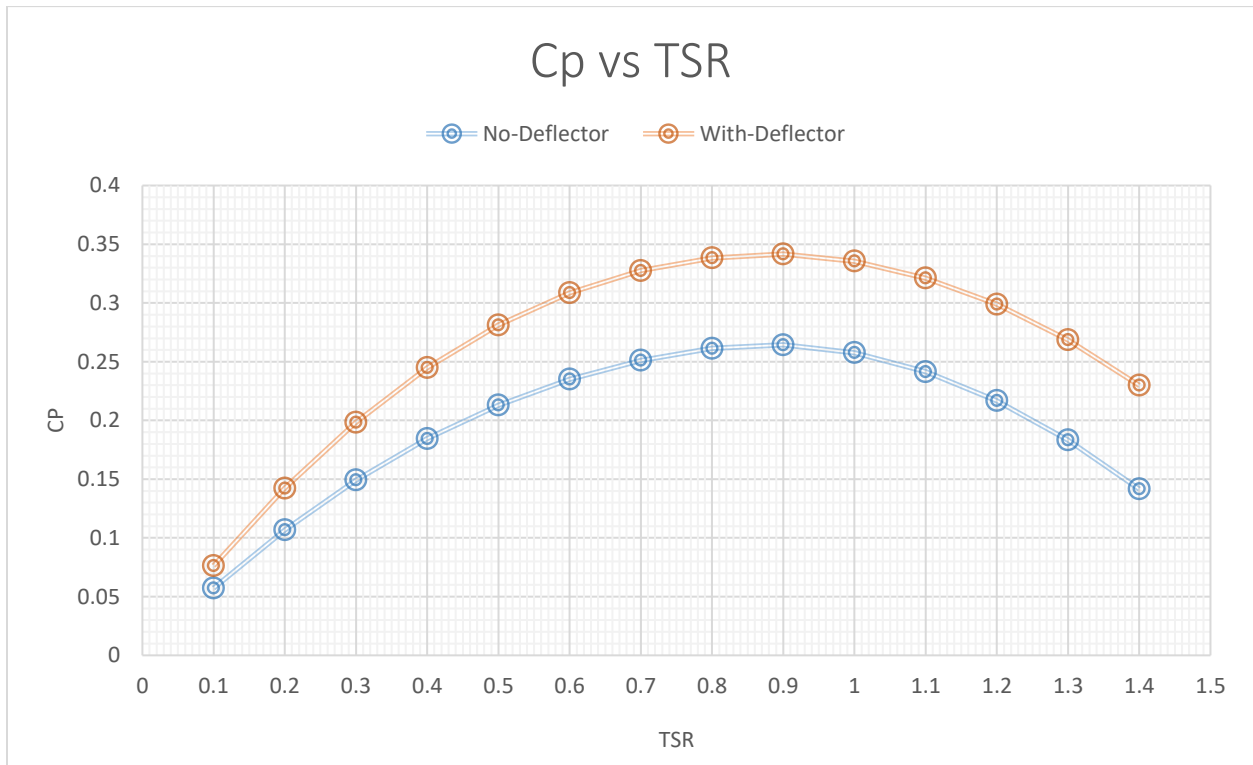


Figure 32: Effect of Deflector

Velocity contours of the turbine are also deduced and are shown in following fig;

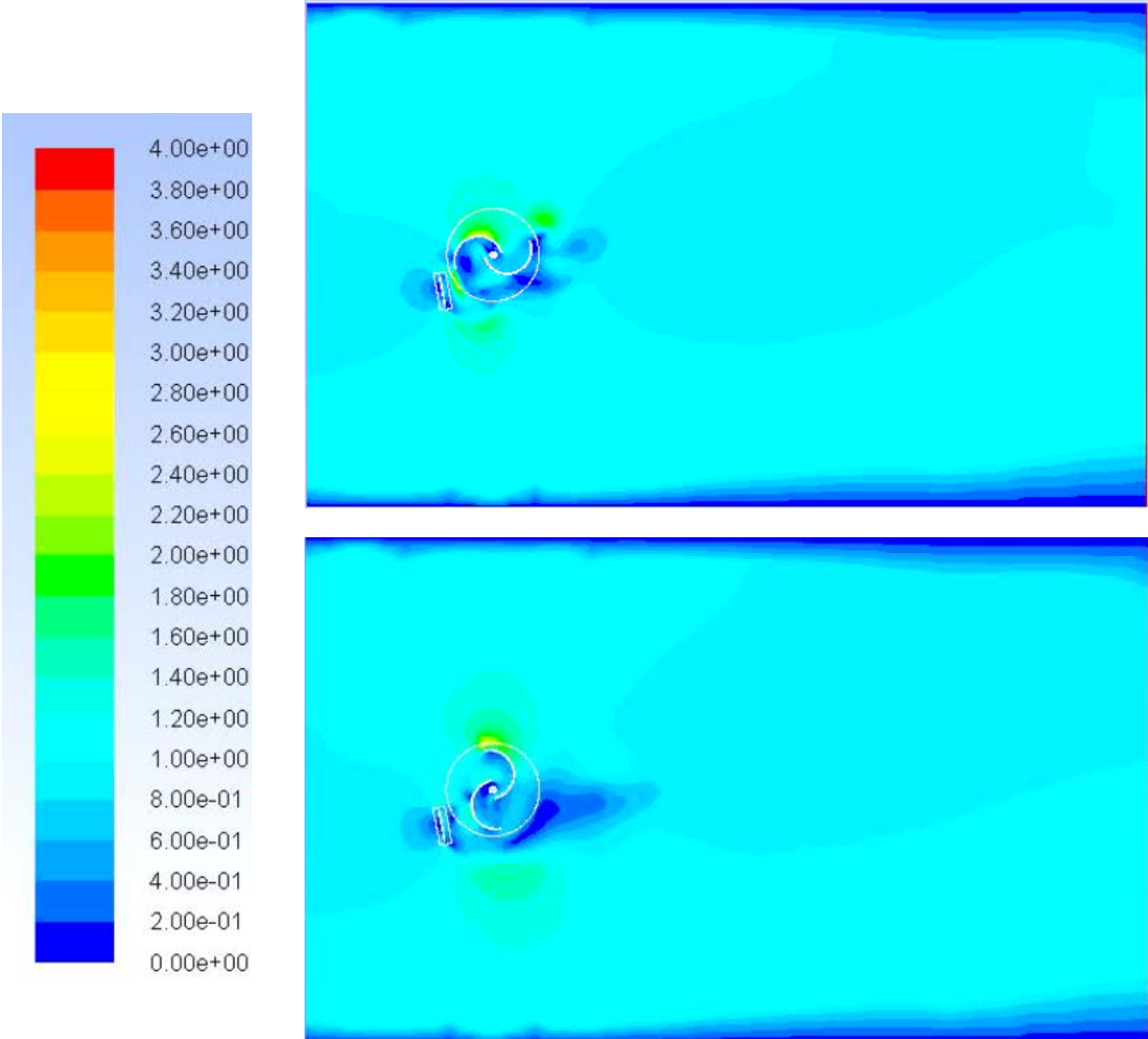


Figure 33: Velocity Contour

4.2 MANUFACTURING

There are few steps in development of a prototype or product. These steps are dependent on each other and are required to be executed in a specific sequence. After the literature review and design, fabrication of the prototype starts. Fabrication is divided into several parts that are discussed below completely.

4.2.1 3D Printing

The most important and most complex part of our rotor is the blade. Because of its unique curvature and the twist, it makes it hard to manufacture it through normal processes. It requires more care and accuracy. Therefore, 3D-printing was used to print all the blades.

The material used in 3D-printing is PLA. PLA material is lightweight thus reduces the torque needed for the turbine to rotate.

4.2.2 Side plates and Frame Fabrication

Side plates are designed so that blades could fit in to it making a tap joint. Acrylic sheet of 2 mm is used to design the side plates. Cavities in side plates are made by laser cutting of acrylic sheet.

Frame is also made by thick acrylic sheet in which rectangular holes are made using laser cutting to fix deflector in it.

4.2.3 Rotor Assembly

Side plates and blades are joined together using chloroform. Side plates are then joined to an aluminum rod by the help of tap joints. Bearing on each side of the rotor is used to hold the rotor while it is rotating. Bearings are fixed in bearing housings that are connected to frame through screws.

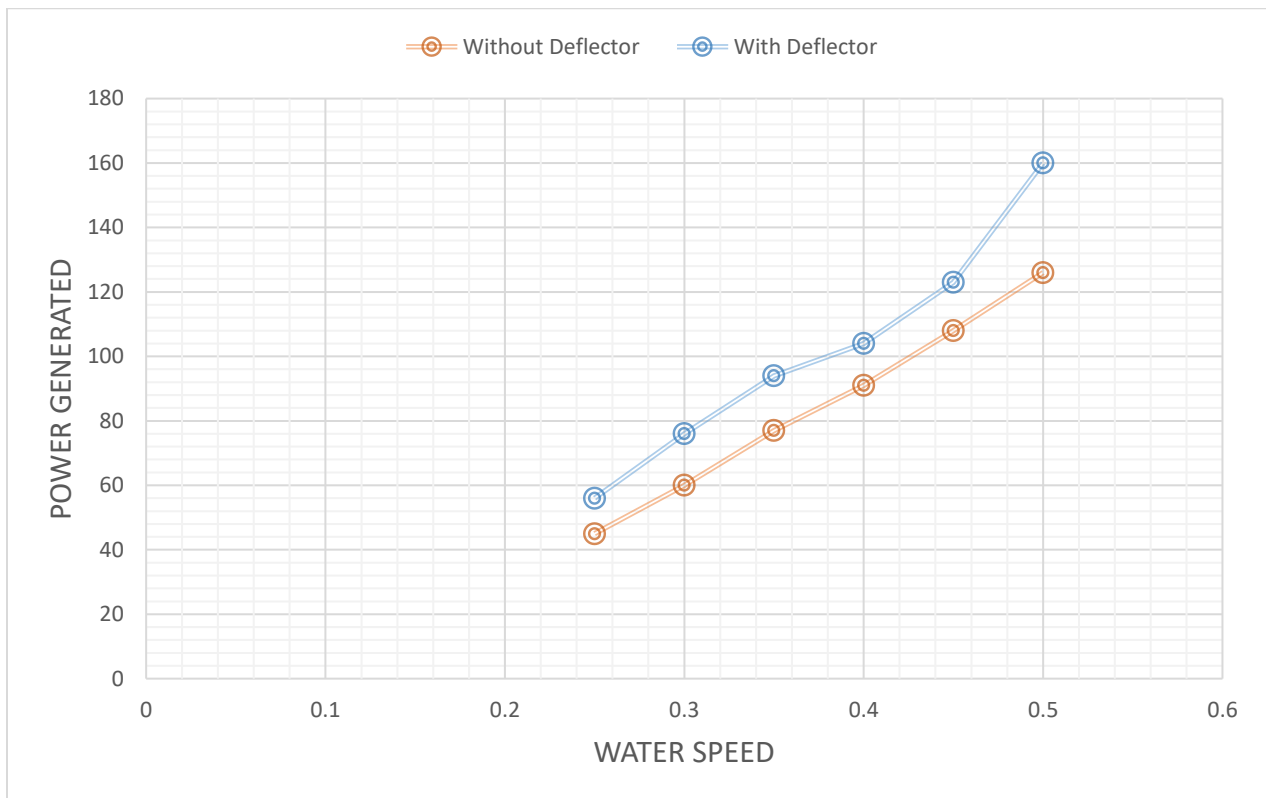
4.2.4 Power Generation Assembly

Gear assembly is used to transmit power from rotor shaft to generator shaft. Single step gear box is used with gear ratio of 0.5. Rotor is rotating at 160 RPM without load and, after generator is mounted rotor rotated at 110 RPM giving 220 RPM to generator shaft.

4.2.5 Calculations and testing

The turbine is tested in the SMME Water tunnel in fluids lab. It is tested several times with and without the power generation assembly. It is also at different water speeds. Water speed is controllable by the motor connected to the tunnel.

RPM of the rotor is used to calculate the RPM of our full sized rotor which was further used to calculate power generated against the water speed. The results are shown below:



CHAPTER 5: CONCLUSION AND RECOMMENDATION

5.1 CONCLUSION

In light of the above-mentioned results, the following can be concluded;

In order to improve the performance of Savonius turbine, numerous studies are carried out. Best possible parameters are chosen for the optimum performance of the devised model. The tests that are performed on ANSYS are very much similar to the trend that already exists in the literature. We conclude following from our results;

5.1.1 Generator Drive Mechanism:

The generator drive mechanism is designed to ensure maximum power transmission, the drive mechanism includes turbine rotor shaft, a pair of spur gears, and generator. In the prototype that is manufactured, gear drive is used while in full scale model belt drive would be used.

5.1.2 Material:

The main concerned material for the fabrication of turbine is the one used in blades. In the prototype PLA material is used in 3D printing of blades. In the manufacturing of full scale turbine rotor blades, Aluminum 6061 is a suitable material for use. It is able to sustain pressure force applied by water and its non-rusting ability makes it a good material for use in river water streams.

5.1.3 Performance:

After incorporating different modifications in a simple savonius turbine following points are concluded for the efficiency and performance of turbine;

- 2 Blade Turbine is more efficient than 3 blade turbine.
- 2-Stages yields more power that single and triple stage.
- End plates results in an increase in output power.
- Deflector plate increases performance by 10%.
- Using overlap ratio increase the performance coefficient by 10%.

Experimental results though on the lower side but still are in very much agreement with the analytical results which makes it safe to assume that the original turbine calculations will prove to be accurate when applied to the larger scale.

5.2 RECOMMENDATIONS

3D printed rotor blades are used in the prototype. It could be future tested with metal casted blades.

The upscaled model of the turbine that we designed could be used in real time solutions. The countless advantages could include use for the electricity supply to the small villages alongside the river streams, use under bridges for free street lights, use in a restaurant near a stream of river for its electricity etc. Thus, there are countless possibilities for the future that lies ahead.

REFERENCES

- [1] Pham L. Riverine Hydrokinetic Technology: A Review. Oregon Tech – REE516 Term Paper; 2014.
- [2] Guney MS, Kaygusuz K. Hydrokinetic energy conversion systems: A technology status review. *Renew Sustain Energy Rev* 2010; 14:2996–3004.
- [3] Khan MJ, Bhuyan G, Iqbal MT, Quaicoe JE. Hydrokinetic energy conversion systems and assessment of horizontal and vertical axis turbines for river and tidal applications: a technology status review. *Appl Energy* 2009;86(10):1823–35.
- [4] Khan MJ, Iqbal MT, Quaicoe JE. River current energy conversion systems: Progress, prospects and challenges. *Renew Sustain Energy Rev* 2008;12 (8):2177–93.
- [5] Kassam S. In-Situ testing of a darrieus hydro kinetic turbine in cold climates [M.S. thesis]. Manitoba, Canada: Dept. Mech. Eng., Univ. of Manitoba; 2009.
- [6] Kamoji MA, Kedare SB, Prabhu SV. Experimental investigations on single stage, two stage and three stage conventional Savonius rotor. *Int J Energy Res* 2008;32:877–95
- [7] Vermaak HJ, Kusakana K, Koko SP. Status of micro-hydrokinetic river technology in rural applications: a review of literature. *Renew Sustain Energy Rev* 2014;29:625–33.
- [8] Khan MNI, Iqbal MT, Hinchey M, Masek V. Performance of Savonius rotor as a water current turbine. *J Ocean Technol* 2009;4(2):71–83.
- [9] Khan MJ, Iqbal MT, Quaicoe JE. River current energy conversion systems: Progress, prospects and challenges. *Renew Sustain Energy Rev* 2008;12(8):2177–93.
- [10] Alexander AJ, Holownia BP. Wind tunnel test on a Savonius rotor. *J Wind Eng Ind Aerodyn* 1978;3(4):343–51.
- [11] Zhao Z, Zheng Y, Xu X, Liu W, Hu G. Research on the Improvement of the Performance of Savonius Rotor Based on Numerical Study. In: *Proceedings of international conference on sustainable power generation and supply (SUPERGEN)*; 2009:p.1–6.

- [12] Iio S, Katayama Y, Uchiyama F, Sato E, Ikeda T. Influence of setting condition on characteristics of Savonius hydraulic turbine with a shield plate. *J Therm Sci* 2011;20(3):224–8.
- [13] Kamoji MA, Kedare SB, Prabhu SV. Experimental investigations on single stage, two stage and three stage conventional Savonius rotor. *Int J Energy Res* 2008; 32:877–95.
- [14] Saha UK, Thotla S, Maity D. Optimum design configuration of Savonius rotor through wind tunnel experiments. *J Wind Eng Ind Aerodyn* 2008;96(8–9):1359–75.
- [15] Damak A, Driss Z, Abid MS. Experimental investigation of helical Savonius Rotor with a twist of 180°. *Renew Energy* 2013;52: 136–42.
- [16] Akwa JV, Vielmo HA, Petry AP. A review on the performance of Savonius wind turbines. *Renew Sustain Energy Rev* 2012; 16(5):3054–64.
- [17] Sivasegaram S. Secondary parameters affecting the performance of resistance-type vertical-axis wind rotors. *Wind Eng* 1978; 2:49–58.
- [18] Jeon KS, Jeong JI, Pan J K, Ryu KW. Effects of end plates with various shapes and sizes on helical Savonius wind turbines. *Renew Energy* 2015; 79:167–76.
- [19] Alexander AJ, Holownia BP. Wind tunnel test on a Savonius rotor. *J Wind Eng Ind Aerodyn* 1978; 3(4):343–51.
- [20] Mahmoud NH, El-Haroun AA, Wahba E, Nasef MH. An experimental study on Improvement of Savonius rotor performance. *Alex Eng J* 2012; 51(1):19–25.
- [21] Kamoji MA, Kedare SB, Prabhu SV. Experimental investigations on single stage, two stage and three stage conventional Savonius rotor. *Int J Energy Res* 2008; 32:877–95.
- [22] Kianifar A, Anbarsooz M. Blade curve influences on the performance of Savonius rotors: experimental and numerical. *Proc Inst Mech Eng Part A: J Power Energy* 2011; 225:343.
- [23] Menet JL, Bourabaa N. Increase in the Savonius rotors efficiency via a parametric investigation. In: *Proceedings of the European wind energy conference & exhibition, London; 2004.*
- [24] Kamoji MA, Kedare SB, Prabhu SV. Experimental investigations on single stage modified Savonius rotor. *Appl Energy* 2009; 86(7–8):1064–73.

- [25] Kamoji MA, Kedare SB, Prabhu SV. Experimental investigations on single stage, two stage and three stage conventional Savonius rotor. *Int J Energy Res* 2008; 32:877–95.
- [26] Hayashi T, Li Y, Hara Y. Wind tunnel tests on a different phase three-stage Savonius rotor. *JSME Int J* 2005; 48(1):9–16.
- [27] Sheldahl RE, Feltz LV, Blackwell BF. Wind tunnel performance data for two and three-bucket Savonius rotors. *AI AAJ Energy* 1978; 2(3):160–4.
- [28] <http://www.brighthubengineering.com/fluid-mechanics-hydraulics/26551-hydraulic-turbines-definition-and-basics/>
- [29] <https://www.sciencedirect.com/science/article/pii/S0306261911001826?via%3Dihub#bi0005/>
- [31] <https://doi.org/10.1016/j.rser.2013.05.006>
- [32] E.N. Jacobs, K.E. Ward, & R.M. Pinkerton. NACA Report No. 460, "The characteristics of 78 related airfoil sections from tests in the variable-density wind tunnel". NACA, 1933.
- [34] <https://doi.org/10.1016/j.aej.2012.07.003>
- [35] <https://doi.org/10.1016/j.renene.2012.10.043>
- [41] [42] <https://doi.org/10.1016/j.apenergy.2011.03.025>